ASPECTS OF THE COMPRESSIBILITY AND AGEING OF PMMA

by A.F.M. Kapteijns

WFW-REPORT 93.170

Eindhoven, October 1993

Supervised by:

Dr. Dipl. ing. R. Wimberger-Friedl
Philips Research Laboratories Eindhoven

Prof. dr. ir. H.E.H. Meijer
Eindhoven University of Technology
Department of Mechanical Engineering

Preface

This project was performed at the research group Polymers and Organic Chemistry of the Philips Research Laboratories Eindhoven in the Netherlands. It is part of a research project on the dimensional stability of injection moulded products. This is the final thesis of my study for the Mechanical Engineering degree at the Eindhoven University of Technology, Department of Fundamental Engineering.

I would like to thank Reinhold Wimberger-Friedl and Hans de Bruin for their support during this work. Furthermore I would like to thank Leo Caspers for his willing ear to listen and for his help. Also I would like to thank my roommates and the rest of the group for their acceptance of me in their midst.

Abstract

In this work the time and temperature dependence of the compressibility of PMMA is investigated. Two different types of experiments were done. The first is a model experiment to determine the (pseudo)compressibility over a wide range of temperatures around the glass transition temperature, T_g. Several samples with different pressures and holding times were measured. The density distribution in the samples is determined with an optical Schlieren measurement method.

A maximum in the densification is observed at the temperature equal to the pressure induced T_g, densification of PMMA starts well below T_g at zero pressure. The different holding times of the pressure had no influence on the density profiles of the samples. The densification of the different samples is not proportional to the pressure applied.

The density is extrapolated to a fictive density profile at zero pressure, from which compressibility relaxation times at a certain temperature interval are determined.

The second type of experiment is injection moulding. From these samples the density profiles were determined in the thickness direction, before and after ageing at different times and temperatures.

The relaxation of the densification is proportional to the original density. After a certain time this results in a U-shaped density profile. With the surface density higher than the core density of the sample.

Table of Contents

Preface ii

Abstract iii

Table of contents iv

Chapter 1 **Introduction** 1
- 1.1 **Objective of the Research** 1
- 1.2 **Thermoplastic Amorphous Polymers** 1
- 1.2.1 The Glass Transition 1
- 1.2.2 Ageing 2
- 1.3 **Choice of Material** 3

Chapter 2 **The Compressibility** 4
- 2.1 **Background** 4
- 2.2 **Calculating the Compressibility** 5
- 2.3 **The Expected Density Variations in the Model Experiment** 6

Chapter 3 **Experimental Set-Up** 8
- 3.1 **The Compressibility Experiments** 8
- 3.2 **The Injection Moulding Experiments** 10
- 3.2.1 The Ageing 11
- 3.3 **The Schlieren Measurements** 12
- 3.4 **The Density Measurements** 14
- 3.5 **The Data Processing** 14

Chapter 4 **Results and Discussion** 15
- 4.1 **The Compressibility Experiments** 15
- 4.2 **The Injection Moulding Experiments** 20
- 4.2.1 the unaged density profile 20
- 4.2.2 the aged samples 22

Chapter 5 **Conclusions and Recommendations** 28
- 5.1 **Conclusions** 28
- 5.1.1 the schlieren equipment 28
- 5.1.2 the compressibility 28
- 5.1.3 the injection moulding experiments 28
- 5.2 **Recommendations** 30
- 5.2.1 the compressibility experiments 30
- 5.2.2 the injection moulding experiments 30

References 31

APPENDICES
- I **the schlieren measurement method** I
- II **the hydrostatic weighing method** V
- III **used equipment** VI
- IV **material characteristics of PMMA, PC, PS** VII

Chapter 1: Introduction

1.1 Objective of the Research

One of the important aspects of the use of organic polymers in functional applications is the dimensional stability. Volume-relaxation and recovery of frozen in strains are processes interfering with the dimensional stability. Volume is directly related to density, which is the subject of this investigation.

In this work the density of several polymer products is investigated with respect to their formation history and/or ageing. It is widely known that the formation history is important for many properties of the polymer in its glassy state. The formation history is characterised by the pressure and temperature course the polymer is subdued to in both the melt and the glass. Different formation paths result in different glasses and therefore in different product behaviour. The compressibility and pseudocompressibility are important parameters for the density profile of injection moulded products. Model experiments are done to determine the (pseudo)compressibility with respect to formation pressure and temperature. A schlieren apparatus is used to measure the density profiles in the samples.

The change of density during physical ageing is measured in injection moulded samples. The focus is on the relaxation of the local densification during processing.

1.2 Thermoplastic Amorphous Polymers

1.2.1 The Glass Transition

Thermoplastic amorphous polymers are used in the glassy state which is a solidified melt. In the melt the polymer maintains its equilibrium in the experimental timescale. With decreasing temperature it departs from its equilibrium. The temperature region at which this departure from equilibrium starts is the glass transition region. In figure 1.1 the polymer behaviour with respect to specific volume is plotted against temperature. In the melt phase
the polymer maintains equilibrium when it is cooled, at a certain temperature the relaxation times become to large to maintain equilibrium so that an excess free volume will be frozen in. Further cooling will increase the relaxation times and the deviation from equilibrium will increase. In the glassy state the polymer follows a straight line with slope equal to the thermal expansion coefficient of the glass, as sketched in figure 1.1.

T_g is not fixed for a polymer but changes under the influence of pressure (p) and

cooling rate (q). T_g increases with the logarithm of the cooling rate and linear with pressure (dT_g/dp) up to 500 MPa, where it becomes constant[Skorodumov, 1]

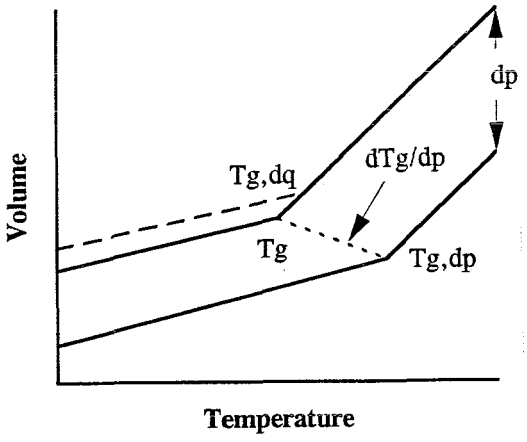

figure 1.1: pVT-diagram

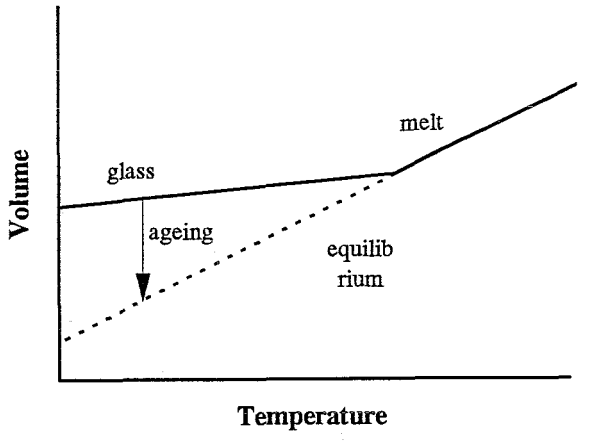

figure 1.2: ageing to equilibrium

During this work the glass transition region is simplified to a single point, the glass transition temperature (T_g). The glass transition is a so-called 2nd order phase transition. Certain properties of the polymer undergo a rapid change, including the thermal expansion and compressibility coefficient. By reheating the polymer above its T_g all history effects will be erased, and the polymer returns to its equilibrium.

1.2.2 Ageing

If the properties of the glass are monitored at constant p and T, one usually observes a slow change in time. This process is called physical ageing[Struik, 2]. The polymer is not at equilibrium in its glass state, but slowly relaxing towards it. At a temperature of only a few degrees below T_g the polymer needs years to reach equilibrium. Ageing is accelerated by a temperature rise of the polymer. The ageing temperature must however stay below T_g because otherwise equilibrium is reached immediately in the melt.

The relaxation rate depends on several parameters. Temperature and the free volume present at the time are the most important. Since the free volume decreases during relaxation (figure 1.2) the relaxation rate is also decreasing. The polymer can only reach equilibrium asymptotically.

The formation history of a polymer affects the ageing too. It was observed by

Greener[3], Wimberger-Friedl[4] and Schenninck[5] that densified polymers first expand before they relax towards equilibrium. In this case the material first relaxes its pressure induced densification before the excess free volume. Since all injection moulded products are made under pressure this is a significant phenomenon for the dimensional stability of polymer products.

1.3 Choice of Material

At the Philips Research Laboratories there is experience with PolyMethylMethAcrylate (PMMA) and PolyCarbonate (PC). At the Philips Competence Centre Plastics b.v. Schenninck[5] has worked with PolyStyrene (PS). For both PS and PC the material characteristics were determined to run simulations with the Holey-Huggings model at the Eindhoven University of Technology.

Because the samples are examined with the schlieren method[6;7;8;9](appendix I), the optical properties are important. PS and PC both have a stress optical coefficient two orders of magnitude higher than that of PMMA. Therefore the influence of birefringence on the optical schlieren method was expected to be too large for both materials.

In the compressibility experiments the expectation was that due to the static type of the experiment, birefringence would be low. Therefore the experiments were done with PC too. First results however, showed that birefringence was still too high.

Therefore all experiments covered by this report were carried out with PMMA 7H from Röhm Gmbh. The material parameters of this material are compared with those of PS and PC in appendix III.

Chapter 2: The Pseudo-Compressibility

2.1 Background

The compressibility κ is defined as,

$$\kappa = -\frac{1}{V_0}\frac{\partial V}{\partial p_{T,p_0}} \qquad (2.1)$$

Where V is specific volume and p the pressure applied at constant temperature T and starting pressure p_0. Figure 2.1 shows a pvT-diagram of PMMA[Kenndaten., 10], from this diagram the compressibility is calculated according to equation 2.1. Figure 2.2 shows that the compressibility changes gradually in the glass and melt. But when passing T_g a rapid change takes place in a small temperature region. The shape of this change has great influence on the densities formed by injection moulding.

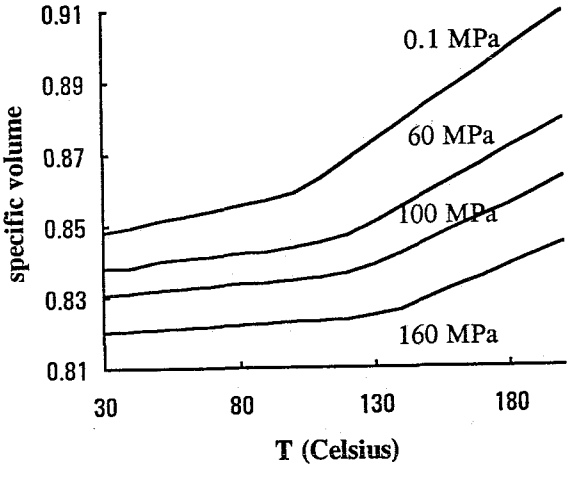

figure 2.1: pvT-diagram of PMMA[Kenndaten., 10]

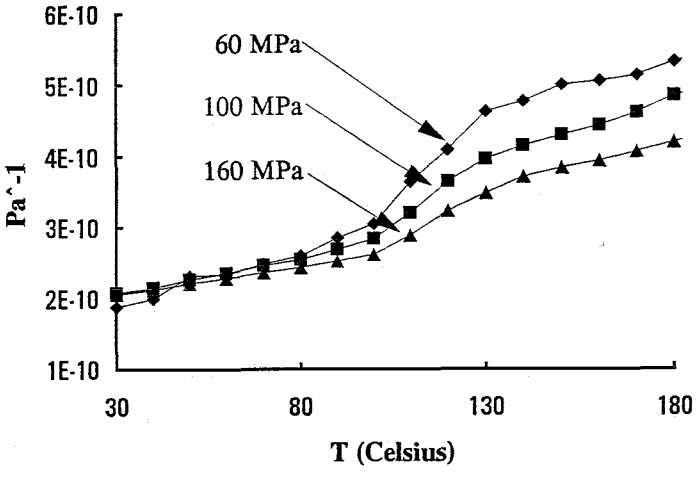

figure 2.1: compressibility derived from figure 2.1

This comes forward in the so-called pseudocompressibility[McKinney et ak, 11] κ', which relates the formation pressure with the residual density of the product.

$$\kappa' = -\frac{1}{V_0}\frac{\partial V}{\partial p_{T,p_0,q}} \qquad (2.1)$$

The subscripts T, p_0 and q denote respectively the initial temperature and pressure and the applied cooling rate. δV is the change in specific volume remaining after the pressure is

released. $\delta V/V_0$ can be replaced by $\delta\rho/\rho_0$, the relative change in density. Mckinney and Simha[11] derived geometrically the following equation for κ',

$$\kappa' = \Delta\alpha\left(\frac{\kappa_g - \kappa_T}{\Delta\alpha} - \frac{dT_g}{dp}\right) \qquad (2.2)$$

were κ_g and κ_T denote the compressibility at respectively the final and initial pressurization temperature and dT_g/dp is the change in T_g with respect to the pressure. Equation 2.2 is written this way to show the relation with the first Ehrenfest relation[11]. Equation 2.2 can be rewritten with κ_T on the left hand side,

$$\kappa_T = \kappa_g - \kappa' - \Delta\alpha\frac{dT_g}{dp} \qquad (2.3)$$

From equation 2.3 it becomes clear that the compressibility can be calculated from the residual compression (=pseudocompressibility)

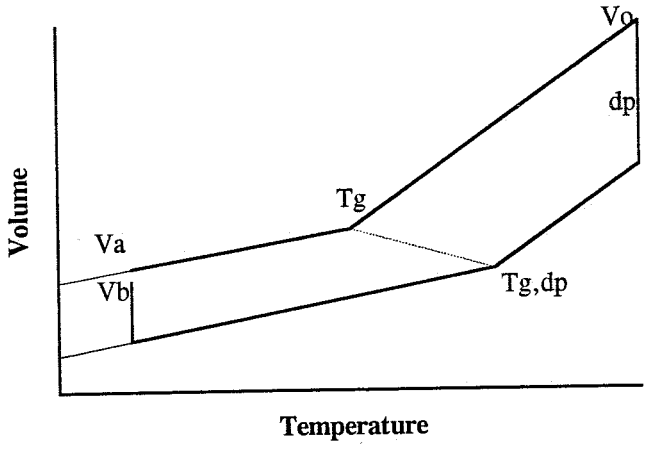

figure 2.3 schematic illustration of a method to obtain a densified glass[11], V_A-V_B = δV

2.2 Calculating the compressibility

Equation 2.2 is only valid if the polymer is pressurized above $T_{g,p}$ and goes through $T_{g,p}$ by means of lowering the temperature. If the polymer undergoes a pressure induced glass transition or if the polymer is not going through T_g at all, equation 2.2 must be modified to deal with the different situations. The region in which a pressure induced glass transition occurs is limited by two temperatures. The lowest temperature is $T_{g,p=0}$ and the highest is the

pressure induced glass transition temperature, $T_{g,p=p}$. In this region the polymer behaves at first as a melt and remains at its equilibrium, but after the passage of the dT_g/dp line (figure 1.1) it behaves as a glass, and should be regarded that way.
When calculating the compressibility for area 1 (figure 2.4) the third part of the right-hand side of equation 2.3 is zero, since there is no $\Delta\alpha$. In area 2 the polymer undergoes a pressure induced glass transition, at one part of the course the polymer is behaving as a melt and at the second part it is a glass, so equation 2.3 is modified to take this into account.

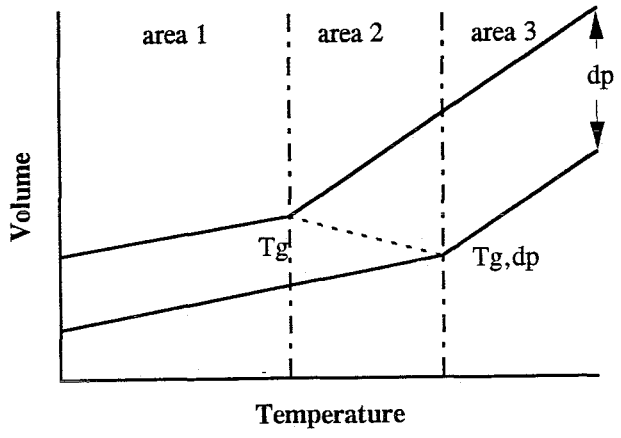

Figure 2.4: different areas for the compressibility calculations

In area 3 only the compressibility at the border can be calculated because at higher temperatures the polymer maintains equilibrium until it reaches $T_{g,p=p}$. Changes above this temperature cannot be calculated from this experiment. Together these arrangements lead to the following set of equations for calculating the compressibility,

Area 1
$$\kappa_T = \kappa_g - \kappa' \tag{2.4}$$

Area 2
$$\kappa_T = \kappa_g - \kappa' - \left(\frac{T-T_g}{T_{g,p=\Delta p} - T_g}\right)\Delta\alpha\frac{dT_g}{dp} \tag{2.5}$$

Area 3
$$\kappa_T = \kappa_g - \kappa' - \Delta\alpha\frac{dT_g}{dp} \tag{2.6}$$

For $\Delta\alpha$, dT_g/dp and κ_g literature values are used, κ' is experimentally determined.

2.3 The expected density variations in the model experiment

Literature values for κ and κ' are known. For polymers pressurized below T_g the residual densification is small. The real densification occurs at $T_{g,p=P}$[Kimmel et al, 12, 13, 14]. The pressurized material above $T_{g,p=P}$ will all have the same densification, because of the ability to maintain equilibrium until $T_{g,p=P}$ is reached. The expected step in the compressibility will occur in the interval between T_g and $T_{g,p=P}$. The interval itself will grow proportional to the applied pressure following equation 2.7,

$$\textit{Temperature interval transition area} = \frac{dT_g}{dp} * \Delta p \qquad (2.7)$$

Kimmel and Uhlman found a densification of 1.5% at 190°C and a pressure of 435 MPa. The pressures used in our experiments are lower, the expectation for the densification is therefore lower then this value.

Chapter 3: Experimental Set-Up

3.1 The compressibility experiments

The PMMA granulate is dried for two days at 90°C under vacuum and after that pressed into discs of 30 mm diameter and 2 mm thickness. Eight discs are melted together in a cylindrical mould (figure 3.1) to form one cylindrical sample of 16 mm height. The sample is put in the same mould and put in the press where a temperature gradient is established over the sample. Between all these steps the samples were kept in a vacuum oven at 90°C.

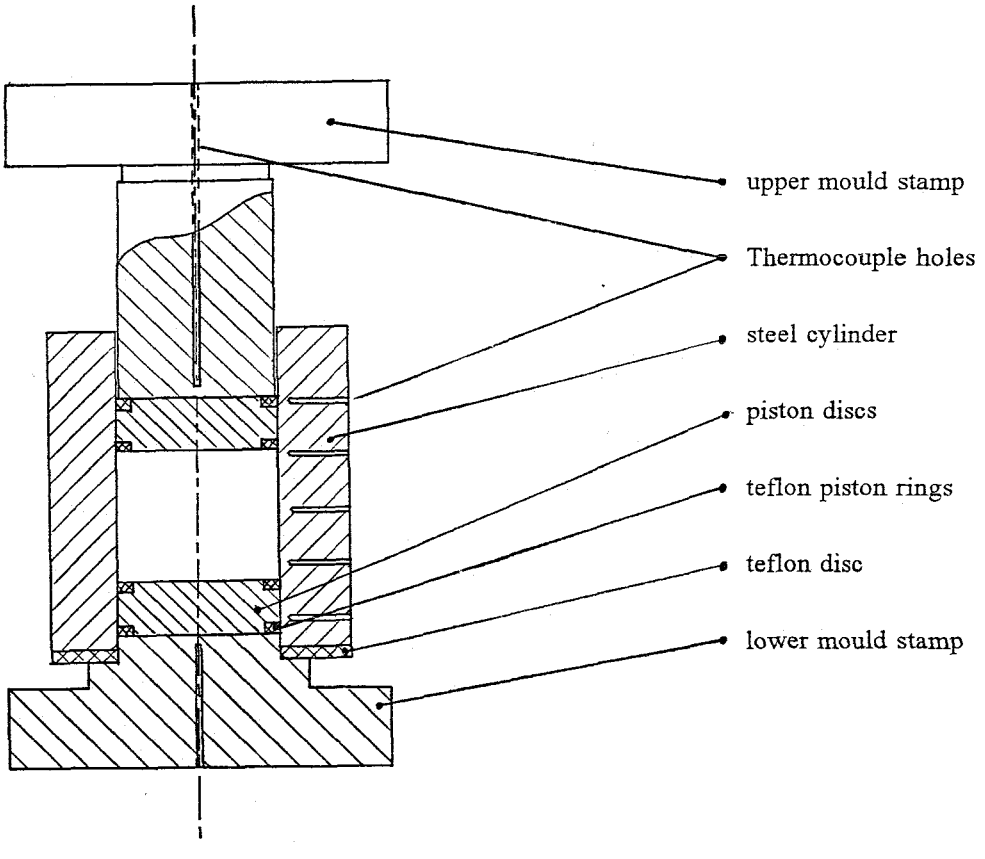

Figure 3.1: the cylindrical mould

The cylinders are pressurized in a steel cylindrical mould between two plates of a Fonteyne flat plate press. The temperatures of the upper and lower plate can be set independent of each other, the two plates are connected serial to the cooling unit. An extra cooling facility for the lower plate was made to cool this plate to lower temperatures so that the temperature gradient in the sample was high enough for our purposes.

The sample was heated to 200°C and kept there for half an hour. Then the heating of the lower plate was switched off and the cooling switched on to establish a temperature gradient of about 60°C over the sample.

The cooling was monitored by hand because no automatic cooling programme can be installed at the press. By adjusting the temperature regulation of the upper plate every 4 minutes a constant cooling rate is established. In table 3.1 the specific temperatures and pressures for each sample are documented.

Because the majority of the heat flow passes through the mould and not through the sample attention must be paid to the radial heat flow in the sample. The radial heat loss must be minimized to get a homogenous temperature over the radius. After applying the temperature gradient to the sample, half an hour is waited to minimize the radial temperature gradient before applying pressure. To prevent a significant radial temperature gradient during cooling, typical cooling rates of only 1°C per 4 minutes were used leading to estimated temperature differences over the radius of 2°C at the most.

To minimize the loss of heat in radial direction two cylinders are placed around the mould. The inner one is constructed from two polyimide cylinders that can slide along each other. This prevents heat loss by convection. The outer one is made from aluminum to reduce the radiation heat loss. The bottom of the cylinder rests on three bulbs to reduce axial heat flow to the plate. With the aid of these improvements it was possible to create a temperature gradient of 5°C/mm over a sample of 16 mm height.

name	pressure applied(Pa)	holding time (hours)	T_{bottom} (°C)	T_{top} (°C)	q (°C/min)	Remarks
PT00	0	0	70	135	0.25	
PT40	57	1	70	135	0.25	
PT460	57	2	73	127	0.25	
PM70	99	0	71	152	0.25	
PM760	99	1	72	145	0.25	The pressure was released at 90°C at the top.
PM7120	99	2	68	145	0.25	
PM140	198	0	63	153	0.25	

Table 3.1: The settings of the compressibility experiment

The force of the press is read out in tons, with a maximum of 20 tons. 1 Ton at the press corresponds to 14 MPa pressure in the sample. In this way a maximum pressure of 280 MPa can be established. The accuracy of the press is 1 to 2 tons.

After installing a new press, with no separate cooling for the lower plate, the experiments were modified in this way that the samples are made homogeneous before they enter the press and the heating of the lower plate was not put on in the beginning of the experiment. In this way also a temperature difference of 50 degrees was established over the sample. The force is read out in kN with an accuracy of 0.1 kN.

After the sample is cooled down to room temperature the pressure is released and the sample is taken out of the mould. Then a cross section is cut out for the schlieren measurements (figure 3.2). After that three pieces are cut out of the cross section to measure the absolute density in a density gradient column. With these values the density profile is established.

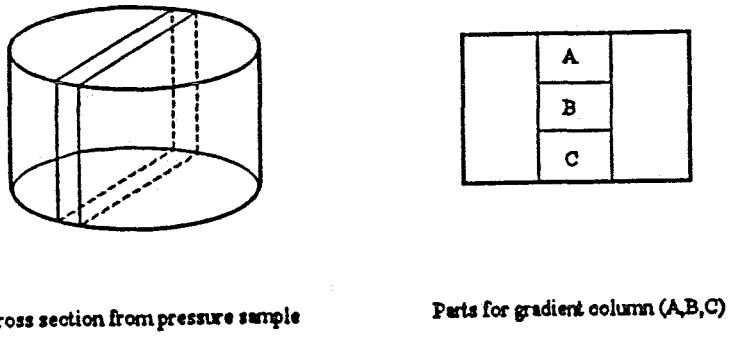

Figure 3.2: the cross section and parts for the gradient column of the compressibility experiments

3.2 The Injection Moulding Experiments

For the injection moulding of the samples an Arburg 35 ton press is used with the flat plate mould. Figure 3.3 shows how the cross sections and the pieces for the hydrostatic weighing and the gradient column are cut out of the injection moulded products.

The injection moulding settings are documented in table 3.4. The pressure profiles printed as + xx% indicate an increasing holding pressure starting at the percentage mentioned from 50 bar and increasing in the first half of the holding time to 50 bar. In appendix IV the recorded pressure during injection moulding is documented. In the last column the

experiments corresponding with Wimberger-Friedl's experiments three years ago are shown. The last two samples were made with different filling conditions.

sample name	injection velocity (cm/s)	mould temperature	holding pressure	pressure profile	RWF sample
bk1	10	30	0		RWM 18
bk2	10	30	30		RWM 19
bk3	10	30	50		RWM 20
bk4	10	30	50	+ 80%	
bk5	10	30	50	+ 40%	
bk6	1	30	50	+ 40%	
bk7	3	30	50	+ 40%	
bk11	10	60	0		RWS 2
bk12	10	60	30		RWS 1
bk13	10	60	50		RWS 3
bk15	10	60	50	+ 40%	
bk16	10	60	50	+ 0%	
bk17	1	60	50		
bk21	10	90	0		RWM 4
bk22	10	90	30		RWM 5
bk23	10	90	50		RWM 6
bk25	10	90	50	+ 40%	
bk26	10	90	50	+ 0%	RWM 8
bk27	0.5	90	50	+ 0%	filling time 2 s
bk28	0.5	90	50	+ 0%	filling time 5 s

Table 3.2: The settings of the injection moulding experiments

3.2.1 The Ageing

The pieces cut out of the injection moulded product are aged at several temperatures and during several ageing times. The different ageing times and temperatures are documented in table 3.3.

At first three pieces of six settings were aged at two different temperatures. They were

measured at the mentioned time intervals and put back in the oven for further ageing. After the pieces were taken out of the oven they got one hour to cool to room temperature before they were measured.

Next, two cross sections were aged according to table 3.3 and measured at different time intervals with the schlieren equipment. After this four cross sections and 32 pieces were aged at four temperatures for one or two hours. These combined measurements result in absolute density profiles for the injection moulding samples.

3.3 The schlieren measurements

All cross sections of both the compressibility and the injection moulding experiments are measured with the schlieren equipment described in appendix I. The magnification for the measurements is adjusted to the different sizes of the samples.

For the cross sections of the compressibility experiments of 16 to 20 mm wide, the magnification chosen is one, resulting in lenses f_1 and f_2 of 120 mm. The sample of 20 mm width is measured in two parts which overlap each other.

The injection moulding cross sections are 2 mm wide, lenses f_1 and f_2 are chosen respectively 120 and 300 mm, resulting in a magnification of 2.5. The density profiles are measured at 8, 72, 88 and 105 mm from the end of the cavity. The positions 8, 72 and 105 are at the same distance as the pressure transducers (figure 3.3).

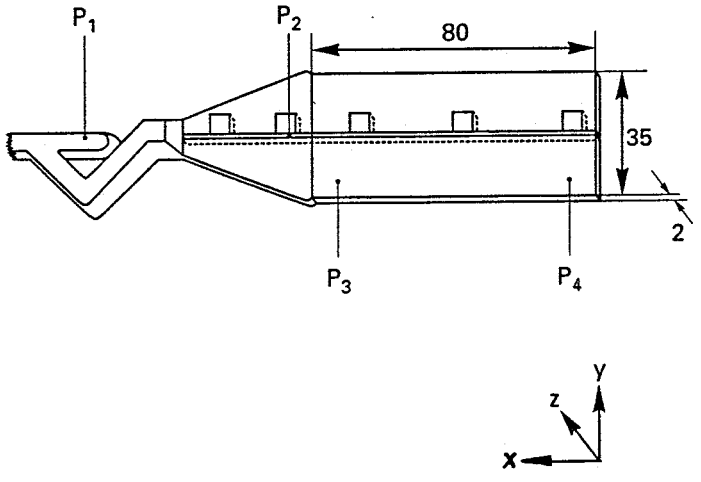

Figure 3.3: the flat plate mould

The cross-sections are immersed in ((48-52%) dimethyl-phenylmethylsiloxane copolymer 125 cs) with a refractive index of 1.50. The refractive index of pressureless-cooled PMMA at 20°C is 1.49. With densification of the sample the refractive index will increase so that the differences between the immersion fluid and the PMMA will decrease. In this way variations of the thickness over the sample, with a maximum value of 10 μm, result in a maximum error of 10% (appendix I) of the refractive index variations.

Samples	Position mm	Ageing Temperatures °C	Ageing Times hours	Cross section	Piece
bk1	8, 72, 88	70, 80 70 80	0, 1, 3, 8, 27 115, 339 163, 523		X
bk3	8, 72, 88	70, 80 70 80	0, 1, 3, 8, 27 115, 339 163, 523		X
bk13	8, 72, 88	70, 80 70 80	0, 1, 3, 8, 27 115, 339 163, 523		X
bk16	8, 72, 88	60, 70 60 70	0, 1, 3, 8, 96, 312 27, 115, 339		X
bk23	8, 72, 88	70, 80 70 80	0, 1, 3, 8, 27 115, 339 163, 523		X
bk26	8, 72, 88	60, 70 60 70	0, 1, 3, 8 96, 312 27, 115, 339		X
bk1	8, 72, 88, 105	70	0, 1, 3	X	
bk3	8, 72, 88, 105	80	0, 8, 27, 72, 480	X	
bk12	8, 72, 88, 105	60, 90	0, 1, 2	X	X
bk13	8, 72, 88, 105	70, 80	0, 1, 2	X	X

Table 3.3: Ageing times and temperatures

3.4 The density measurements

Absolute density measurements were carried out with the hydrostatical weighing method[15](appendix II). A Sartorius 2002 MP1 balance is used, accurate to 0.0001 gram. The water temperature is measured with a chromium-alumel thermocouple accurate to 1°C. In the aged pieces a hole was made before ageing, with the aid of a 0.1 mm fish thread the pieces are positioned in the balance. To measure the absolute density of some pieces with greater precision a gradient column filled with a K_2CO_3 solution was used.

3.5 The data processing

The gradients of the refractive index in the samples are stored on diskettes and later processed with a specially written programme on a Hewlett-Packard computer. Every measurement contains 256 values equally spaced over the height of the sample. These dn/dz values are transformed, with equation AI.9, to dρ/dz values and after that integrated to a density profile.

The compressibility sample coordinate is replaced with a temperature scale equal to the temperatures in the sample at the moment of pressurizing. The slopes of the density profiles measured with the schlieren equipment were not in agreement with the density measurements done in the gradient column. Therefore the slopes of the schlieren measurements were adjusted to the gradient column measurements.

The tilt introduced by the schlieren equipment to the profile of the injection moulded samples is neutralized under the assumption that the core profile is symmetric. There is no reason why this should not be the case, both sides of the mould have the same temperature and the mould itself is also symmetric. The average density of the samples is measured in the gradient column and assigned to the average from the schlieren measurement. If no average value is determined the schlieren average is given the value of 1 g/cm^3. These results are compared with each other and the results from Wimberger-Friedl. They are discussed in the next chapter.

Chapter 4: Results and Discussion

4.1 The Compressibility Experiments

Figure 4.1 shows the measured density profiles of four samples vitrified under different pressures. The densities determined by the gradient column are also shown. The highest and lowest gradient column values are used to calculate the slope of the schlieren density measurements. Good agreement is seen between the third gradient column values and the calculated profiles. All samples have roughly the same density at the cold side, within $1*10^{-3}$ of 1.1975 g/cm^3. None of the samples cooled under pressure has a lower density then the zero pressure sample. At the high temperature end the densities of samples differ, but less then is expected in advance. This has great consequences for the pseudocompressibility. The density profile shows a maximum at $T_{g,p=P}$, and a slight decrease towards higher temperatures.

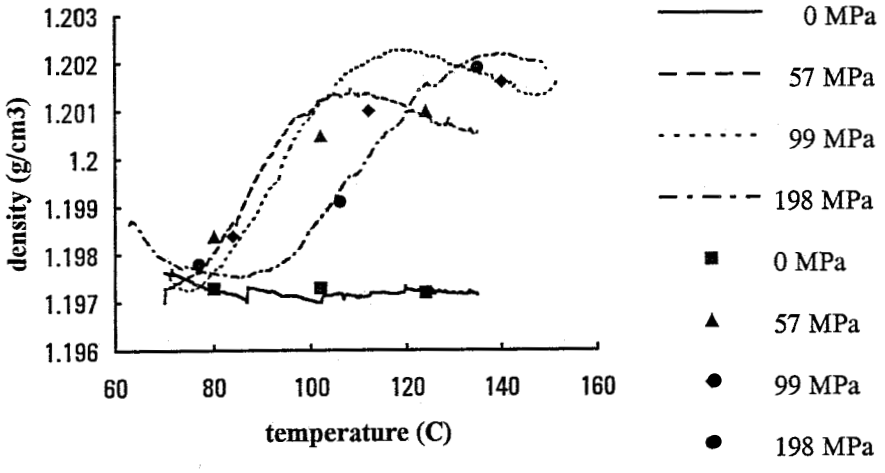

figure 4.1: The density profiles of four samples against formation temperature

The density profiles are reduced to their density change, the lowest density is assigned the value zero. The temperature at 20% densification intervals is plotted for each pressure in figure 4.2. Also the 1-1/e % densification is calculated and printed. According to equations 2.4-2.6 the maximum densification occurs at $T_{g,p=\Delta P}$. This is confirmed by the maximum densification temperature shift, which is 0.23°C/MPa, what is equal to literature values of dT_g/dp[11].

There is a linear relation between the applied pressure and the percentage densification in the samples. The densification rates are extrapolated to 0 MPa (figure 4.2) to loose the

effect of the T_g shift on the densification (equation 2.6). In this way a densification profile is established which depends only on the compressibility relaxation times at the different temperatures (figure 4.3).

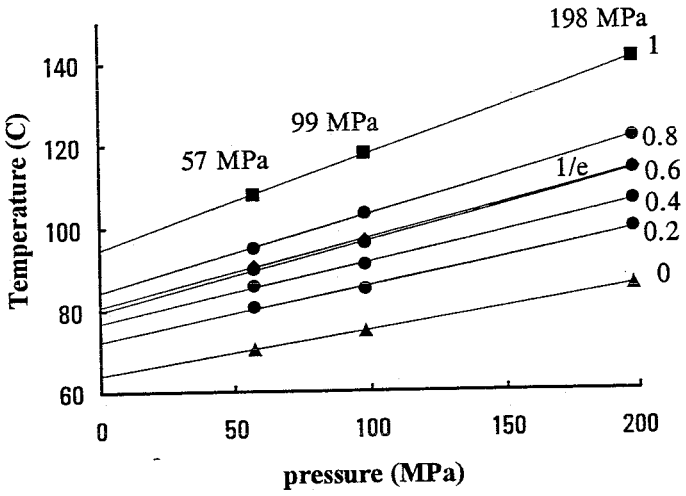

figure 4.2: densification percentage against pressure and temperature

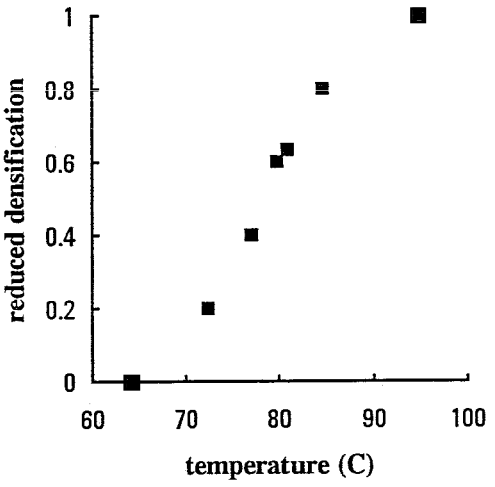

figure 4.3: reduced densification at 0 MPa

The 1-1/e % densification is assigned the relaxation time of 1 hour, being a typical time for the experiments done. With equation 4.1 relaxation times of six other temperatures were calculated and shown in figure 4.4.

$$(1-\exp-(\frac{t_0}{\tau})^{\beta})*100 = \%\ densification \qquad (4.1)$$

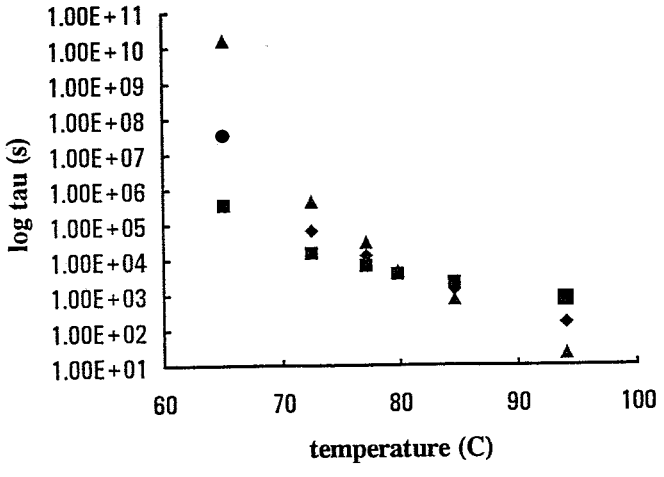

figure 4.4: compressibility relaxation times at different temperatures at an extrapolated pressure of 0 MPa for three values of ß (■, ß=1; ◆, ß=0.5; ▲, ß=0.3)

Figure 4.4 shows τ for ß values of 0.3, 0.5 and 1. ß=1, indicating only one relaxation time, shows little change in τ with temperature. O'Reilly[22] found ß values between 0.3 and 0.45 in DSC measurement, indicating a broader spectrum of relaxation times. These values show a greater temperature dependence of τ (figure 4.4).

In the zero pressure sample no density variations were found in the vertical as well as in the horizontal direction. Therefore the variations in the other samples are solely dependent on the applied pressure.

Different density profiles were found over the diameters of the samples, near the side the density variation was much smaller then in the core. This indicates that the applied pressure was not homogeneous throughout the sample. The polymer sticks to the wall of the mould introducing shear stresses. These extra stresses absorb a part of the applied force near the wall in this way causing a lower compression. Two different measurements indicate that the influences of the shear stresses are practically zero at 5 mm from te wall, leaving an inner part with 20 mm diameter where a homogeneous pressure condition was present during the experiment.

When making the samples from different discs some dust was captured between the discs. These lines of dust show a U-profile after the experiment is done, indicating the sticking of the polymer to the mould wall. The inner 20 mm of the lines are horizontal and parallel to each other indicating a homogeneous pressure condition.

Also the schlieren measurements differ the most in the outer 5 mm. The profiles measured in the inner 20 mm all show no significant differences. All measurements used in this work are taken from the core of the samples.

The birefringence in the samples is not constant. In three of them birefringence measurements are done across the height along the axis in the cross-sections. The highest values, about 10^{-6}, are recorded in the area were the density changes the most. If unpolarized light is used the maximum error is equal to 1/6 of the total birefringence variation along the scanning direction[4]. With density variations of order 10^{-3} the influence of the birefringence can be neglected.

Figure 4.5 shows the pseudocompressibility calculated from the distributions in fig 4.1, with equation 2.2. κ' is not the same for the various pressures applied. The maximum pseudocompressibility varies with pressure, indicating a non linear relationship between the pressure and the densification. The compressibility itself becomes smaller at higher pressures[3]. According to equation 2.3 this results in smaller values for κ'. This can account for the fall in κ' at higher pressures. Earlier reports[4] described a linear relation for pressures

below 80 MPa. The pressures used here are 60, 100 and 200 MPa and are above that range. The κ' values for 60 and 100 MPa are in reasonable agreement with literature data, at 200 MPa it is only half of the lowest data found.

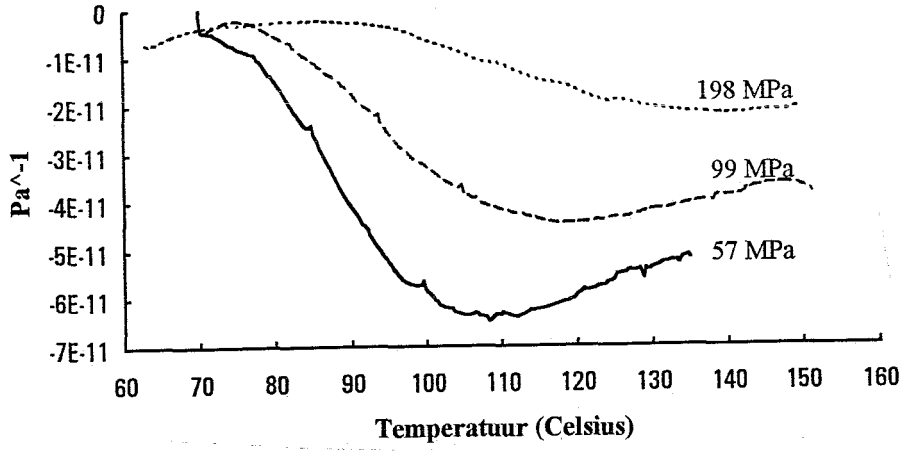

figure 4.5: Pseudocompressibility against the temperature at pressurization

The maximum κ' shifts to higher temperatures at higher pressures, corresponding with the T_g shift. Parts undergoing a pressure induced T_g transition are harder to densify below $T_{g,p}$ in their glass state. At $T_{g,p=\Delta P}$ the first deviation from equilibrium starts. In the area 2 between T_g and $T_{g,p=\Delta P}$ the PMMA first maintains its equilibrium and after passing dT_g/dp the deviation from equilibrium starts. Material that never reaches T_g (area 1) never reaches equilibrium, still even in this area a densification occurs. So it is concluded from these results that PMMA can be densified without being brought above T_g. The first signs of densification shift to higher temperatures with increasing pressure. The PMMA at higher temperatures has a slightly lower pseudocompressibility. A part of the decreasing κ' values at high pressures can be explained by the decreasing κ at rising pressures.

This means that for literature values of both κ and κ', the pressure by which these values are found should be mentioned.

The compressibility is calculated from the measured pseudocompressibility with equations 2.4-2.6 and shown in figure 4.6. Above $T_{g,p=\Delta P}$ (area 3) the compressibility shows a plateau, this is expected because during the cooling the PMMA keeps its equilibrium until it reaches $T_{g,p=\Delta P}$.

The course of the compressibility is very much similar to literature values[10]. A discrepancy of less then 10% is found for the 60 and 100 MPa samples. No data on 200 MPa was found to compare with.

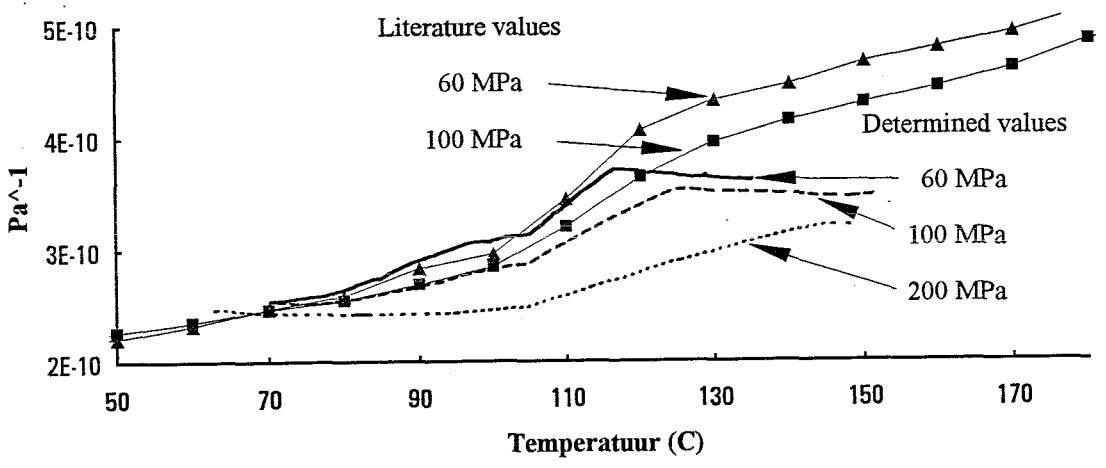

figure 4.6: compressibility values calculated with equation 2.4-2.6 from the experiments and literature values derived from Kenndaten.., [10]

The width of the compressibility step between the glass and equilibrium values depends on the pressure applied, higher pressures cause a broader step. The width of the glass transition itself is of minor importance for the compressibility step. It is possible if the pressure rises and falls fast that a polymer in injection moulding goes through T_g in both directions before it passes T_g finally.

Most models predict residual stresses that are higher then experimentally found[Douven, 16]. One of the reasons can be that areas with higher stresses have the opportunity to relax by compressing neighbouring areas. This process causes lower stresses near the wall.

When the compressibility step is modelled to take place at one temperature instead of a broad range of temperatures, it is inevitable that the compressibility is underestimated just below T_g and/or overestimated just above T_g. In both cases the predicted residual stresses are to high.

From the results of the experiments it is clear that the reproducibility of the experiments is accounted for. On the other hand it was the goal of this research to determine the way in which the compressibility is time dependent. Due to the small differences found in the samples made by different holding times, it is not possible to estimate the time dependence. Cooling took about five to six hours and the holding times varied between zero and two hours. This means the pressure on the hot side of the sample was applied between two and four hours in equilibrium. Kimmel and Uhlman[12,13, 14] found that the densification increases during the first half hour of the pressure course at $T_{g,p=\Delta P}$. Longer times resulted in no extra densification.

4.2 The Injection Moulding Experiments

The density profiles of the injection moulded samples are investigated with the schlieren method. After a number of samples had undergone an accelerated ageing programme, the density profiles were measured again. Also some samples made by Wimberger-Friedl three years ago were measured to compare with the new samples.

4.2.1 The Unaged Density Profile

In figure 4.7 a typical density distribution of a injection moulded PMMA sample is depicted. As one can see there a density peak beneath the surface. This peak is caused by the fact that the material in this place is vitrified under a higher pressure than the core material. The change in profile along the sample is caused by the different pressure histories during moulding, see pressure tracks in appendix IV. The core material at position P3 and P2 vitrifies under higher pressures than that at P1, while the density maximum is almost unaffected.

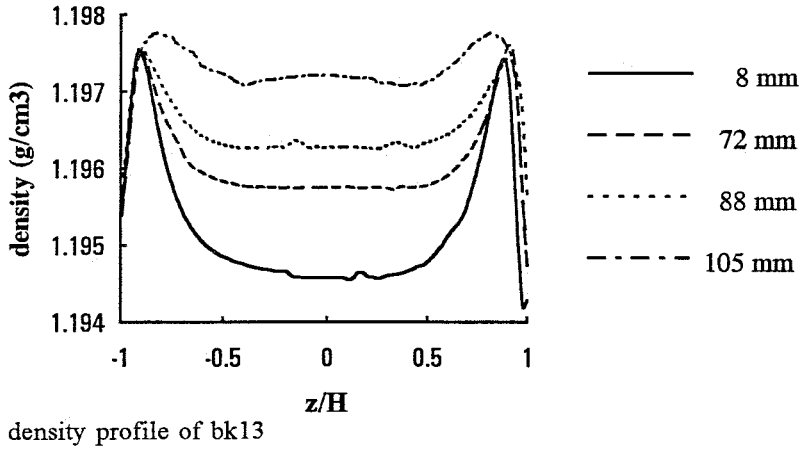

figure 4.7: density profile of bk13

If a plus pressure profile is applied, a second peak (figure 4.8) can be seen in the density profile a bit more inward as the first. This second peak, or preferably the density minimum between both peaks, originates from the drop in pressure after filling the mould and the rise of the pressure thereafter. It can be concluded that the first density peak is caused by the rapid cooling of the first PMMA arriving in the mould under filling pressure and the second peak by the holding pressure. If the pressure is kept at a certain fixed level after filling, the first and second density peak fluently coincide with each other and no minimum is seen.

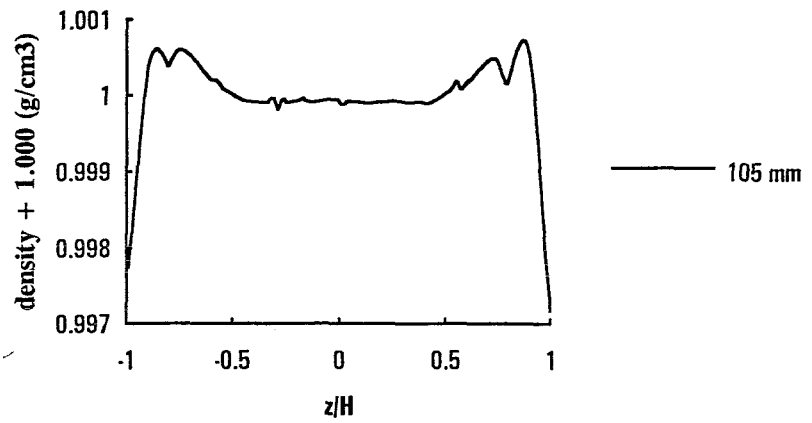

figure 4.8: density profile of bk17

The level of holding pressure had no influence on the slope of this peak. All samples, having the same slope in the density profile at the surface, have the same filling conditions. If the injection velocity is lowered (samples bk6, bk7, bk17, bk27) the slope towards the peak is decreasing.

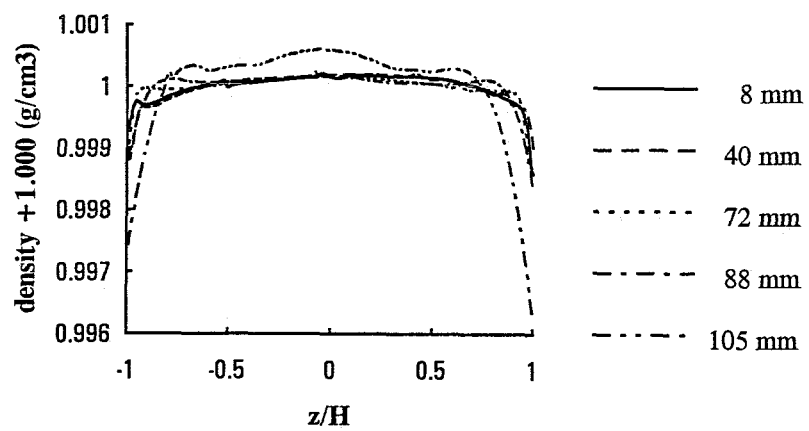

figure 4.9: density profile of bk26

Higher holding pressures cause higher vitrification pressures and broadening of the peaks at the inside and a higher core density. If the mould temperature is raised too, it is possible to vitrify the core with a higher density as the peaks (figure 4.9, bk26). It comes forward that the core density is principally determined by the holding pressure and the mould temperature.

The surface seems to have the same density for all the samples. This is difficult to confirm experimentally because the integration boundary of the schlieren measurement cannot be placed more accurately than within 0.01 mm on the surface of the sample. In this area of the

density profile a displacement of 0.01 mm is a change in density of about $5*10^{-4}$ g/cm^3. All determined surface densities are within $1*10^{-3}$ g/cm^3 of each other. Also the density of the zero pressure compressibility sample is within this range. This confirms Wimberger-Friedl's conclusion that the surfaces are vitrified under zero pressure conditions.

Wimberger-Friedl[4] shows that the residual stresses in injection moulded PMMA are to small to explain density variations higher than $1*10^{-4}$ g/cm^3. He also found birefringence values, of $2*10^{-4}$. Under the assumption of a biaxial medium and if unpolarized light is used the error made in the refractive index variation is 1/6 of the birefringence variation. The error in the density values is in the order of a few percent. Measurements with polarised light showed no significant difference in the refractive index profiles.

4.2.2 The Aged Samples

Because the densities cannot be measured in the oven during ageing but only at room temperature a heating and cooling course is introduced. The influence of these courses is neglected since the ageing rate rapidly decreases with temperature. A consequence of these courses is that short ageing times cannot be regarded since in that case the heating and cooling courses become significant. The samples were stored 2 to 4 hours before the density measurements were done. A few pieces of the samples were aged at 70°C and 80°C to determine the course of the average density during ageing.

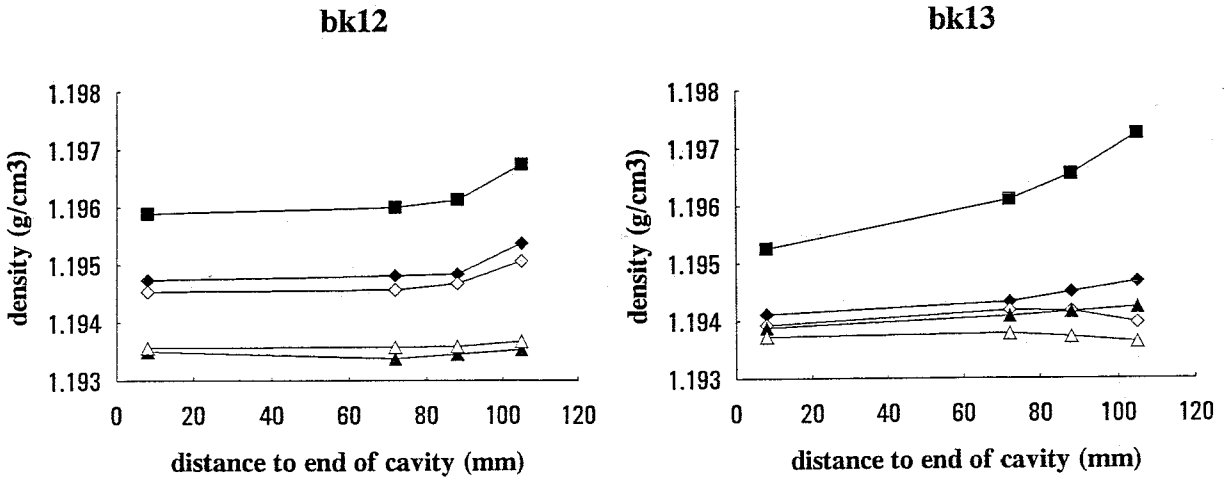

figure 4.10: The gapwise averaged density along the injection moulded plates of bk12 and bk13 during ageing. (bk12), ■, unaged; ◆, 1 hour , 60°C; ◊ 2, 2 hours, 60°C; ▲, 1 hour , 90°C; △, 2 hours, 90°C; (bk13), ■, unaged; ◆, 1 hour, 70°C; ◊, 2 hours, 70°C; ▲, 1 hour 80°C; △, 2 hours, 80°C;

Two cross sections were aged to look for changes in density profiles. For this purpose cross sections from two different samples were used, 2 x bk12 and 2 x bk13. The cross-sections from bk12 were aged at 60°C and 90°C, both cross-sections from bk13 at 70°C and 80°C. The ageing times were chosen at 1 and 2 hours.

The pieces cut out of the injection moulded samples bk12 and bk13 followed the same ageing programme as the cross sections and their densities are measured in the gradient column. With these values the schlieren measurements can be translated to absolute instead of relative density profiles.

As can be seen in figure 4.10 the density of the injection moulded plates is increasing from the end towards the gate. Upon ageing the average density decreases and the variation becomes less pronounced. Somewhere between one and two hours aging at 80°C the density at the gate becomes lower than at the cavity end of the sample. This indicates some kind of overshoot in the density relaxation. At 90°C the density distribution is almost flat after one hour and after two hours the expansion is turned into a shrinkage to equilibrium. It seems that the pressure relaxation is already done at this stage.

The results of the Schlieren measurements in the cross-sections are shown in figure 4.11 and 4.12. The surface of the samples seems to keep the same density during ageing with an accuracy of $1*10^{-3}$. All the other parts of the samples show expansion instead of shrinkage. This is due to the fact that the samples are vitrified under pressure. The density peak decreases during ageing and just between the surface and the peak a density minimum comes forward. This is caused by the different material history of the surface and the inside of the sample.

The relaxation is proportional to the densification of the sample as can be seen in figure 4.13 where the relaxation profiles are shown. These relaxation profiles are calculated by subtracting the density profile after ageing from the original density profile.

The striking resemblance between the relaxation and the density profile indicates a relation between the pressure during vitrification and the relaxation. The peak in the relaxation profiles coincides exactly with the density peak giving further evidence to this relation. The first expansion of the samples is a pressure relaxation. After a certain time interval the free volume relaxation becomes bigger and the expansion changes to shrinkage towards equilibrium. The relaxed density profiles show that the core density also decreases, indicating a significant formation pressure there. Even if the original core density is lower than at the surface the density decreases so that the difference between both places becomes bigger.

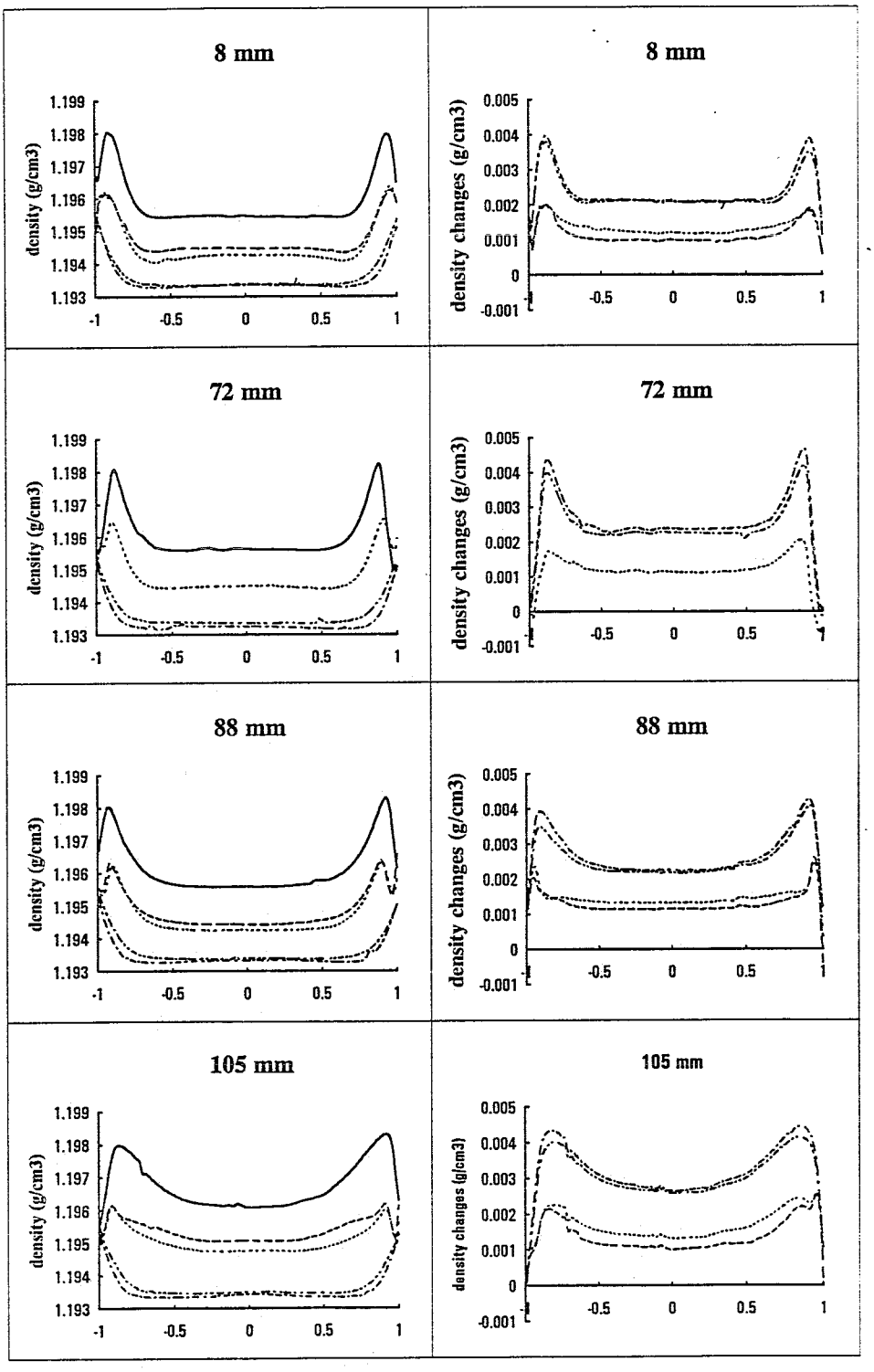

figure 4.11: bk12 aged at 60°C and 90°C during one and two hours, density profiles on the left side and relaxation profiles on the right side (-, unaged; --, 1 hour 60°C; ... 2 hours 60°C; -.- 1 hour 90°C; -..- 2 hours 90°C)

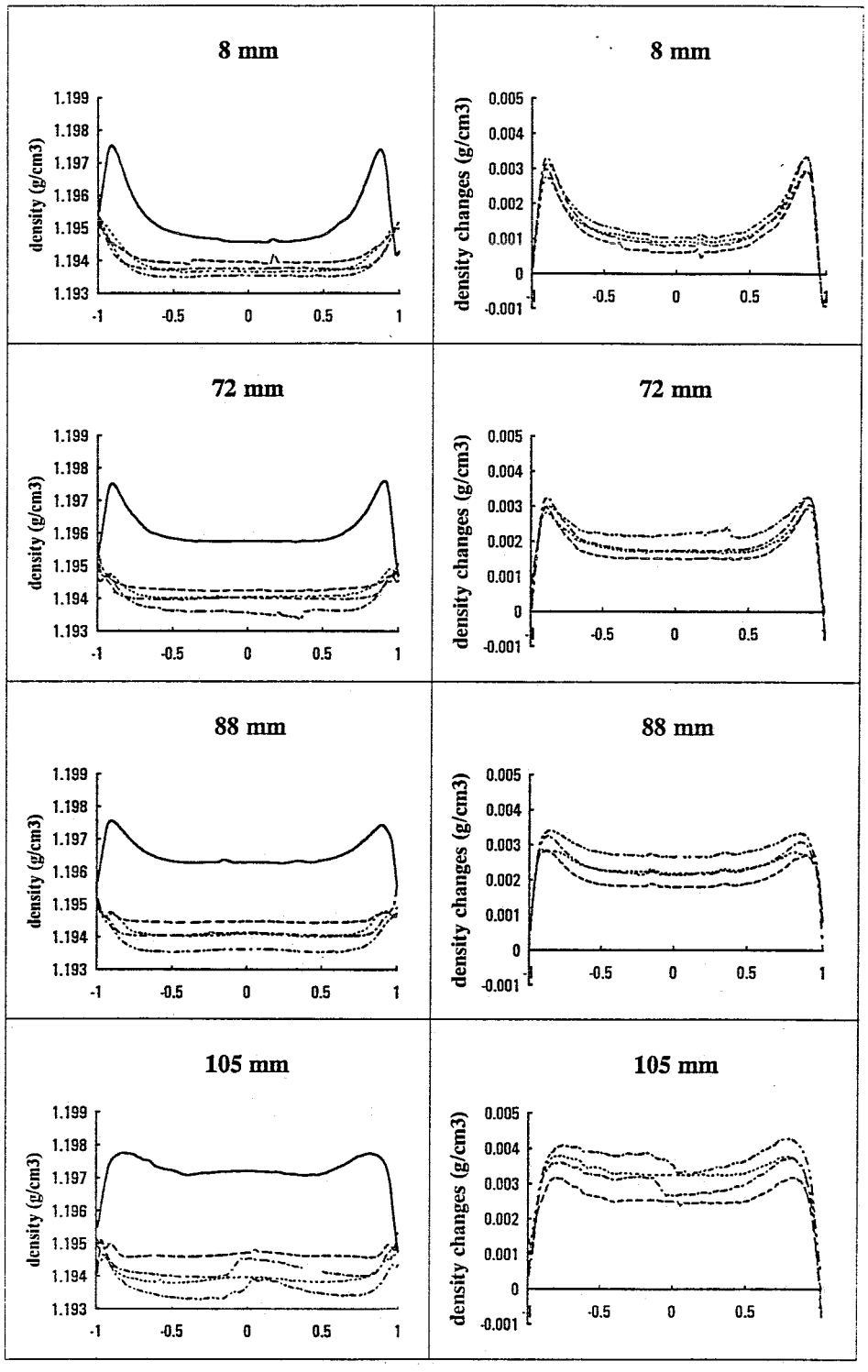

figure 4.12: bk13 aged at 70°C and 80°C during one and two hours, density profiles on the left side and relaxation profiles on the right side (-, unaged; --, 1 hour 70°C; ... 2 hours 70°C; -.- 1 hour 80°C; -..- 2 hours 80°C)

The density profile, resulting from two hours ageing at 90°C, shows a U-shaped core density that is lower than the surface density. This profile was also found in other samples aged at 70 and 80°C. One sample was aged for 480 hours at 80°C and still had this same density profile. A proper explanation for the fact that the density at the surface is about $2*10^{-3}$ g/cm^3 higher than in the core is not found yet.

One reason for this higher surface density could be the silicon oil, which is used as an immersion liquid for the schlieren measurements. At the ageing temperatures the oil that sticks to the surface might diffuse into the sample, thereby causing an increase in density. But when the silicon oil is able to diffuse over 0.25 mm in two hours, it also must be able to diffuse 1 mm in 480 hours. Since this did not happen another explanation must be looked for.

The experiments done with pieces of the samples which are aged at 70°C and 80°C indicate that after more than 550 hours the average density starts increasing. As shown in figure 4.13 there is a pressure relaxation in the first stage of ageing covering two to three decades in time. There is no fundamental difference between the relaxation of the samples moulded under different conditions. At 80°C the pressure relaxation already started after 30 minutes, whereas at 70°C it seems to start between 30 minutes and 1 hour. Schenninck simulated the pressure relaxation for PS and PC and found similar profiles as those in figure 4.13.

Since the hydrostatic weighing method is not more accurate than $2*10^{-3}$ g/cm^3 the exact density changes could not be determined, but the global density changes are monitored well enough to support the above conclusion, especially since all pieces show the same relaxation effects at the same temperatures.

The density profiles of the cross sections made three years ago differ not much from those of the unaged samples. The same profile is still there but density differences between the peak and the surface or core are about half of the original differences. This supports the conclusion that the first relaxation is proportional with the pressure induced density, since the profiles show the same density distribution. The density profiles of the samples moulded now with the same settings as three years ago show the same profiles as those measured by Wimberger-Friedl three years ago.

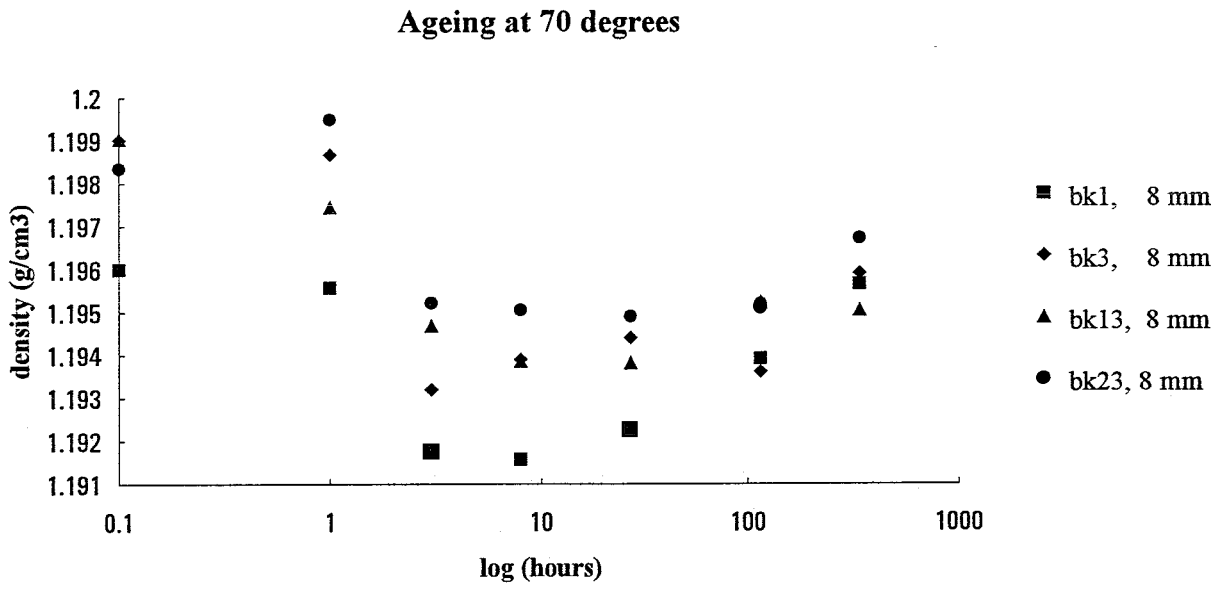

figure 4.13: density against ageing time at 70°C of bk1, bk3, bk13, bk23, bk16 and bk26. measured with the hydrostatic weighing method.

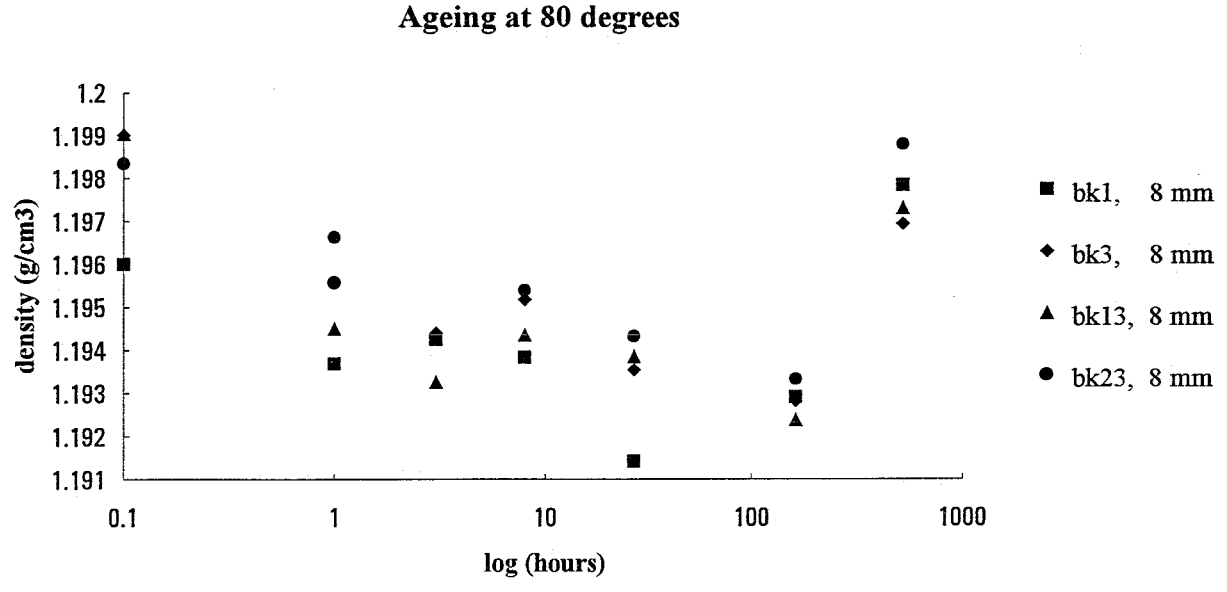

figure 4.14: density against ageing time at 80°C of bk1, bk3, bk13, bk23, bk16 and bk26. measured with the hydrostatic weighing method.

Chapter 5: Conclusions and Recommendations

5.1 Conclusions

5.1.1 The Schlieren Equipment

- With the schlieren equipment relative density profiles of amorphous polymers can be accessed easily. There is always an extra measurement needed to determine the absolute density profile.

- The polymers measured with the schlieren equipment must meet certain demands with respect to the optical quality. The stress optical coefficient must be low. must be small.

5.1.2 The Compressibility Experiments

- The pseudocompressibility is not proportional to the formation pressure. At higher pressure the pseudocompressibility drops. This is the same for the compressibility and therefore not unexpected. One consequence is that any value of the (pseudo)compressibility without mentioning the pressure at which it is determined cannot be compared with other values. This probably is one of the reasons why literature values vary so much between each other.

- In the temperature area below $T_{g,p=\Delta P}$, κ' changes rapidly with the temperature to a maximum value at $T_{g,p=\Delta P}$.

- The interval in which the densification step occurs increases with pressure. The densification starts at higher temperatures if a higher pressure is applied.

- If the densification profiles at different pressures are extrapolated to 0 MPa, the influence of the T_g shift is left out and just the relaxation times of the compressibility are left.

- Within the applied range the different holding times of the pressure had no influence on density profiles of the samples. Therefore they had no influence on the pseudo compressibility and the compressibility.

- The densification of PMMA starts well below T_g and reaches a maximum at $T_{g,p=\Delta P}$.

- The equations 2.4-2.6 are a correct way for calculating the compressibility up to $T_{g,p=\Delta P}$ as can be seen from the good resemblance between literature and experimental values.

- The reproducibility of the experiments is good. The differences between two experiments with the same pressure applied can hardly be seen.

- A homogeneous pressure condition over the whole sample cannot be reached in the cylindrical mould. If only inner parts, with a 20 mm diameter, of the samples are taken in account the pressure condition can be regarded as homogeneous.

5.1.3 The Injection Moulding Experiments

- Density profiles of polystyrene and polycarbonate cannot be measured with the schlieren method, without a correction for birefringence effects

- Average density variations in the samples are caused by the variations in the core density. The different moulding parameters have little or no influence in the density of the outer shell of the samples, with respect to the mould temperature which is of great influence for height of the density peak below the surface. The surface of the samples is vitrified pressureless.

- The height and place of the density peak under the surface is determined by the mould temperature and the filling injection speed.

- The density relaxation is proportional to the original residual compression of the samples. The density relaxation profile has the same shape as the density profile. Also the cores of the samples relax.

- At 80°C an overshoot in the density relaxation is seen. More densified parts relax to lower densities than the parts vitrified under a lower pressure.

- At 90°C the shrinkage of the samples starts within two hours. The pressure relaxation is already over at that time and temperature.

- The results from hydrostatical weighing are not precise enough to calculate an absolute density profile. Therefore gradient column values must be used, which are one magnitude more precise.

5.2 Recommendations

5.2.1 The Compressibility Experiments

- The timescale of the experiments must be adjusted to establish a density difference between the different experiments to determine the time dependence of the compressibility at the same pressure. A comparison between the relaxation times determined in this report and those can be made.

- The experiment must be run with shorter cooling times, some experiments with zero pressure samples must be done to see if this affects the density distribution in height or radius.

- It would be interesting to measure the ageing of the compressibility samples to see how they relax and if an overshoot in the expansion occurs at the more densified parts.

5.2.2 The Injection Moulding Experiments

- Some research should be done to the effect of the filling stage on the density profiles just under the surface.

- Ageing experiments with the cross sections should be extended to longer times and the absolute density profiles at longer times should be determined. Especially interesting is de development of the U-profile in the samples, and if, and when the sample has a homogeneous density.

- More density relaxation profiles must be determined so that shift factors for the pressure relaxation at different temperatures can be calculated.

References

[1] V.F. Skorodumov and Yu. K. Godovskii, *Polym. Sci. U.S.S.R.*, Ed., **29**, 127 (1987)

[2] L.C.E. Struik, *Physical aging in amorphous polymers and other materials,* publ. Elsevier, Amsterdam, (1978)

[3] J.J. Tribone, J.M. O'Reilly and J. Greener, *J. of Polym. Sci., Polym. Phys.* Ed., **27**, 837 (1989)

[4] R. Wimberger-Friedl, *PhD Thesis, Eindhoven University of Technology*, (1991)

[5] G.G.J. Schenninck, *Thesis, Eindhoven University of Technology*, (1993)

[6] G. Prast, *Philips Tech. T.* Ed., **43**, 203-210, (1986)

[7] A. Kurstjens and G. Prast, *Quantitative Schlieren optics,* Nat. Lab. Report 6204, (1987)

[8] A. Kurstjens and G. Prast, *Basic transmissive Schlieren system,* Nat. Lab. Report 6365, (1989)

[9] M. Idzes, *Realisatie van een schlieren opstelling voor de mechanische afdeling van het Philips Natuurkundig Laboratorium, nr. 90112,* (1990), in Dutch

[10] J. E. McKinney and R. Simha, *J. Res. Nat. Bur. Stand., Phys. and Chem.*, Ed., **81A**, 283 (1977)

[11] *Kenndaten für die Verarbeitung thermoplastischer Kunststoffe*, Part 1: Thermodynamik, publ. VDMA; Hanser; Munich, Vienna, (1979)

[12] R. Kimmel and D. Uhlman, *J. of Appl. Phys.*, Ed., **42**, 1892, (1971)

[13] Kimmel and D. Uhlman, *J. of Appl. Phys.*, Ed., **41**, 2917, (1970)

[14] Kimmel and D. Uhlman, *J. of Appl. Phys.*, Ed., **42**, 4917, (1971)

[15] Brown R., *Handbook of Plastic Test Methods*, Ed., **3**, Longman Scientific & Technical, Essex, England, (1988)

[16] Douven L, *Phd. Thesis, Eindhoven University of Technology,* (1991)

[17] Waxler R.M., Horowitz,D. Feldmann,A., *Appl. Optics,*, Ed., **18**, 101 (1979)

[18] Vleeshouwers S.V.M., *Phd. Thesis, Eindhoven University of Technology,* (1993)

[19] Brandrup J., Immergut E.H., *Polymer Handbook*, 2e edition, Publ. John Wiley & Sons, New York, London, (1975)

[20] Rodriguez F., *Principles of Polymer Systems,* 3e edition, Publ. Hemisphere Publishing Corporation, New York, London, (1989)

[21] PBNA, *Polytechnisch Zakboekje,* (1987)

[22] O'Reilly J.M., *CRC Critical Reviews in Solid State and Materials Science,* Vol. 13, Issue 3, (1987)

Appendix I: The Schlieren measurement Method

With the Schlieren optical equipment it is possible to measure refractive index variations in transparent objects. Foucault designed this measurement method in 1859 to control astronomical mirrors on irregularities. The name 'schlieren' method originates from measurements Töpler did in 1884. He visualised refractive index variations in air, caused by density variations. The german word for these air strings is 'Schliere' and is since then used to identify this method.

The schlieren equipment

The equipment is schematically reproduced in figure AI,1. A lightsource S directs light on lens L_1, which directs it to the object. After passing the object lens L_2 focusses the light in S'. Lens L_3 projects the light on the detector, in our case a CCD camera. Between the lenses L_2 and L_3 a knife can be put in the beam ot the light. When put in exactly halfway, half of the light is captured by the knife. The intensity measured by the CCD camera is in that case half of the original intensity. If however a non homogeneous object, with respect to the refractive index, is placed between lenses L_1 and L_2 the beam of light will be diverted differently from every place according to its particular refractive index gradient. Consequently, more or less than half of the intensity of the light passing through that point will be blocked by the knife. In this way the intensity measured at the detector a refractive index gradient can be determined.

The lightsource is a 12 V/ 50 W halogen lamp. In front of the lamp a frosted glass is situated to create a homogeneous source. The lenses have a diameter of 30 mm, providing a physical limitation to the objects measured. Two lens settings are used in this research, documented in table AI-1, for the compressibility experiments and for the injection moulding cross sections. The CCD camera is a Fairchild CAM 1840 with 2590 diodes of 10 μm x 10 μm. The diode array covers physically 26 mm, which is near the maximum beam width the lenses can provide anyway.

The schlieren method

Four measurements are needed to calculate a refractive index profile of a sample. First two reference measurements without object are done, with and without the knife in the light path. After that both measurements are repeated with the object in place.

If the object measured is optically perfect, the knife will block half of the light and

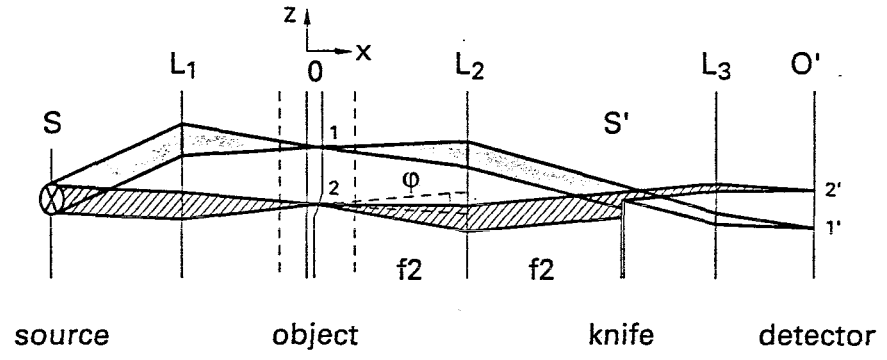

figure AI.1: schematic set-up of the schlieren optical system

the intensity on the diode array will be half of the unblocked value. If however there is agradient in the optical path of the light, the image on the diode array will be shifted and the intensity shall not be half of its original value. The image will be shifted by,

$$\Delta h = \tan\phi f_2 \approx \phi f_2 \qquad \textbf{(AI.1)}$$

for small ϕ. ϕ denotes the deflection angle caused by the refractive index variations in the object. The change in intesity on the diode array relative to the perfect case is given by,

$$\frac{\Delta I}{I_0'} = \frac{\Delta h}{h/2} = \frac{\phi f_2}{h/2} = \frac{\delta(OP)}{\delta z}\frac{2f_2}{h} \qquad \textbf{(AI.2)}$$

OP represents the optical path lenght which is proportional to the thickness and refractive index. Any change in one of those is reflected in OP according to equation AI.3

$$(OP)(z) = n(z) + n_m(D - d(z)) \qquad \textbf{(AI.3)}$$

n_m represents the refractive index of the surrounding medium, in this case a silicon oil with n=1.50.

Differentiating AI.3 gives,

$$\frac{\delta(OP)}{\delta z}(z) = \frac{\delta n}{\delta z}(z)dz + \frac{\delta d}{\delta z}(z)(n(z) - n_m) \qquad \textbf{(AI.4)}$$

The second term on the right-hand side can be neglected if the samples are perfectly flat or if both refractive indices are the same. In our case the refractive indices differ 0.02 and the thickness variations are at the most of magnitude $1*10^{-5}$ m. Compared with the

measured refractive index gradient of magnitude 10^{-3} and the sample thickness of $1*10^{-3}$, this results in a thickness influence of less than 10% for the compressibility experiments. And for the injection moulding experiments, with thickness variations of $1*10^{-6}$ less then 1%. Therefore these influences are not taken into account for the calculations. The objects are assumed to be perfectly flat. Rewriting equation AI.2 results in,

$$\frac{\Delta I}{I_0}(z) = \frac{\delta n}{\delta z}(z)\,d(z)\,\frac{2f_2}{h} \qquad \textbf{(AI.5)}$$

The above derivation is only valid with perfect optical components and a even light distribution on the object. It is evident that this is not the case. Therefore reference measurements are done with no object in place. These measurements are combined with the object measurements to determine the relative intensity on the diodes as in equation AI.6,

$$M = \frac{I}{I'} - \frac{I_0}{I_0'} = \frac{\delta OP}{\delta z}\frac{f_2}{h} \qquad \textbf{(AI.6)}$$

M is the relative intensity, and I the measured intensity, ' are the measurements without knife and subscript 0 denotes the reference measurements without object. Through the reference measurements the imperfections of the equipment is accounted for, the only requirement is for the diode array to present a signal proportional to the light intensity. The reference measurements are made once at the beginning of the measurement session. That is if the equipment is stable, normally it takes two hours for the equipment to become stable.

The processing of the measurements

The measurements with the schlieren method provide data about the gradient of the refractive index in the sample. These values can be related to the density gradient through dρ/dn.Equation AI.5 can be rewritten with dn/dz on the left-hand side,

$$\frac{\delta n}{\delta z}(z) = \frac{\Delta I}{I_0}\frac{h}{2\,d(z)f_2} \qquad \textbf{(AI.7)}$$

The relation between the density and the refractive index is given by the Lorentz-Lorentz equation,

$$\frac{n^2-1}{n^2+1} = \frac{N_A}{\epsilon_0 M}\alpha\rho \qquad \textbf{(AI.8)}$$

To calculate the density profile dρ/dz is needed, this can be calculated by differentiating equation 2.9[4] and simplifying it to,

$$\frac{\delta\rho}{\delta z} = \frac{d\rho}{dn}\frac{\delta n}{\delta z} \qquad \textbf{(AI.9)}$$

With experimental data from Waxler et al[17] the value is for dρ/dn is calculated to be 2.40 g/cm^3.

	compressibility experiments	injection moulding experiments
f_1	120	120
f_2	120	120
f_3	120	300
magnification	1	2.5

Table AI-1: lens settings used

Literature used

[6] G. Prast, *Philips Tech. Tijdschrift*, **43**, 203-210, (1986)

[7] A.V.M. Kurstjens, G. Prast, *Quantitative schlieren optics*, NAT.LAB Report Nr. 6204, (1987)

[8] A.V.M. Kurstjens, G. Prast, *Basic transmissive schlieren system*, NAT.LAB Report Nr. 6365, (1989)

[9] M.H.M. Idzes, *Realisatie van een Schlieren opstelling voor de mechanische afdeling van het Philps Natuurkundig Laboratorium*, MI 90112, (1990)

Appendix II: The Hydrostatic Weighing Method

The average density of the samples is determined with the hydrostatic weighing method[15]. Pieces are cut out of the samples as shown in figure 3.3.

A Sartorius 2002 MP1 analytical balance, with a resolution of to 0.0001 gram is used. The sample is weighed dry and immersed in water of a known temperature. The density of the sample is calculated from both measurements with equation AII.1.

$$\rho_{sample} = \frac{w_{dry}}{w_{dry} - w_{wet}} \rho_{H_2O} \qquad \textbf{(AII.1)}$$

The estimated maximum error follows from eqaution AII.2.

$$\delta\rho_{sample} = \delta\rho_{H_2O} + \delta w_{dry} + \delta(\Delta w_{dry} + \Delta w_{wet}) \qquad \textbf{(AII.2)}$$

And for this case with samples of maximum 0.5 g the error is,

$$\delta\rho_{sample} = 0.02\% + \frac{0.0002}{0.5} * 100\% + \frac{(0.0002 + 0.0002)}{0.4} * 100\% = 0.16\%$$

The reproducibility for repeated measurements has a maximum error of $2*10^{-4}$ g. With a density close to 1.2 g/cm^3 this results in an error of 1.2 * 0.16% = $2*10^{-3}$ g/cm^3. This is almost in the same magnitude as the variations in the profile. So these values cannot be used to calculate the exact density. But certain trends in the density can be determined this way.

w_{dry}	=	dry weight of the cutout piece
w_{wet}	=	weight of the immersed piece
V	=	Volume
ρ	=	density
Δ	=	absolute error
δ	=	relative error

Appendix III: Material Charateristics of PMMA, PS and PC

In the following table the material characteristics used in this report are documented. For some values an estimation is made out of several data, indicated by ±.

	PMMA	PS	PC
trade name	PMMA 7H	Styron 678E	Makrolon CD 2000
supplier	Röhm Gmbh	Dow Chemical	Bayer
T_g (Celsius)	☞[1] 105 ☞[2] 95	90	143
S.O.C.	± $-6*10^{-11}$	± $-5*10^{-9}$	± $5*10^{-9}$
density (g/cm^3)	☞ ± 1.2	1.05	1.2
refractive index	☞ 1.48	1.59	1.58
α_{glass} (K^{-1}/volume)	± $2.5*10^{-4}$	± $2*10^{-4}$	$2*10^{-4}$
α_{liquid} (K^{-1}/volume)	± $5.7*10^{-4}$	± $5.5*10^{-4}$	
κ_g (Pa^{-1})	$2*10^{-10}$	$2.2*10^{-10}$	
dT_g/dp (K/kbar)	☞[2] 23	30	46

☞ Experimentally determined, [1] refractive index measurements, [2] derived from figure 4.2

Literature used

[10] *Kenndaten für die Verarbeitung thermoplastischer Kunststoffe,* Part 1: Thermodynamik, publ. VDMA; Hanser; Munich, Vienna, (1979)

[19] Brandrup J., Immergut E.H., *Polymer Handbook*, 2e edition, Publ. John Wiley & Sons, New York, London, (1975)

[20] Rodriguez F., *Principles of Polymer Systems,* 3e edition, Publ. Hemisphere Publishing Corporation, New York, London, (1989)

[21] PBNA, *Polytechnisch Zakboekje,* (1987)

Appendix IV: The Pressure Profiles of the Injection Moulding Experiments

This appendix shows the pressure profiles of the injection moulding experiments as recorded at the four pressure transducers as shown in figure 3.3. P3 and P4 are situated in the flat plate part of the mould. P2 is in the divergent section and P1 just before the gate. The cycle time was 1 minute and the holding time 10 seconds.

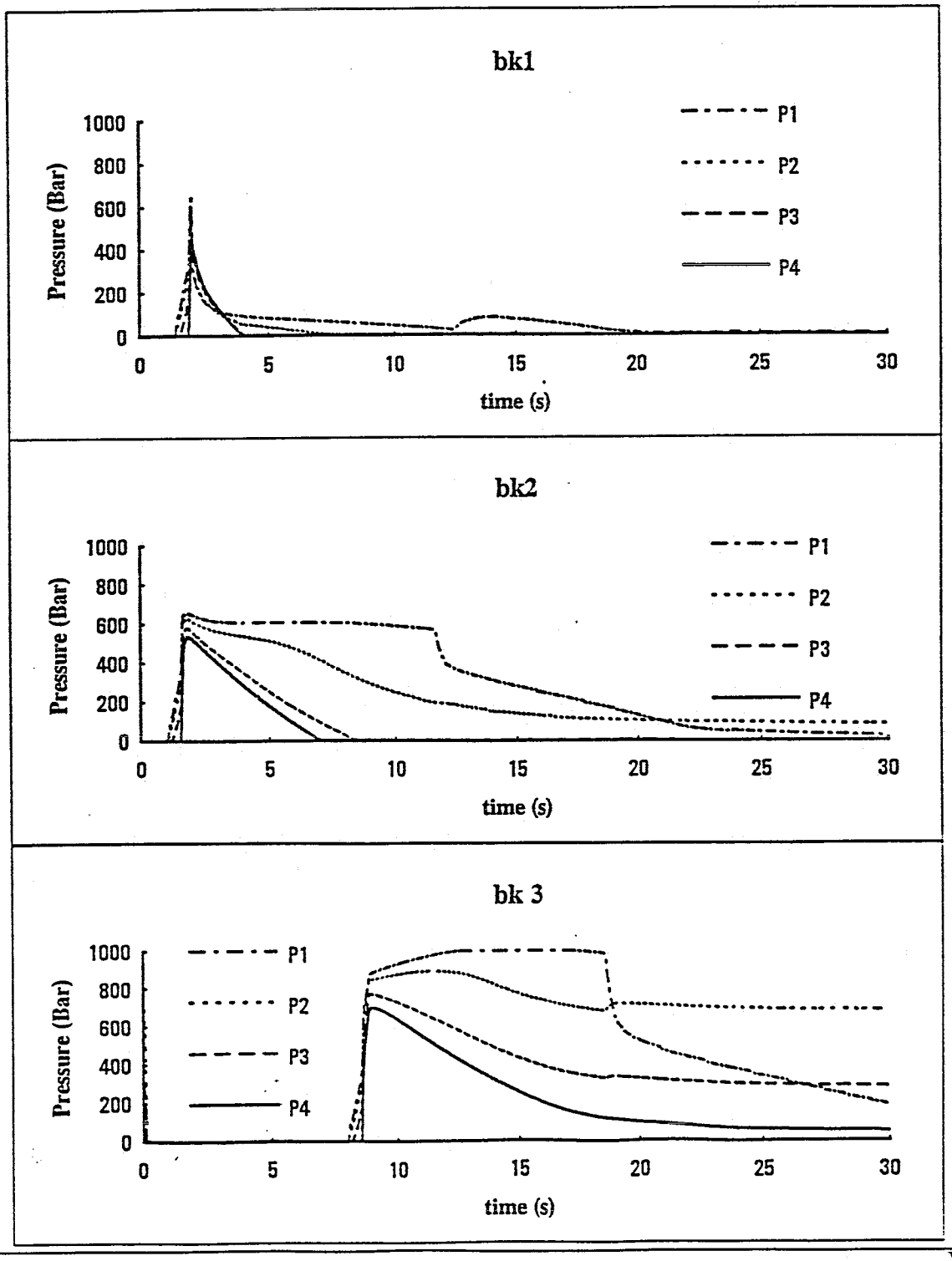

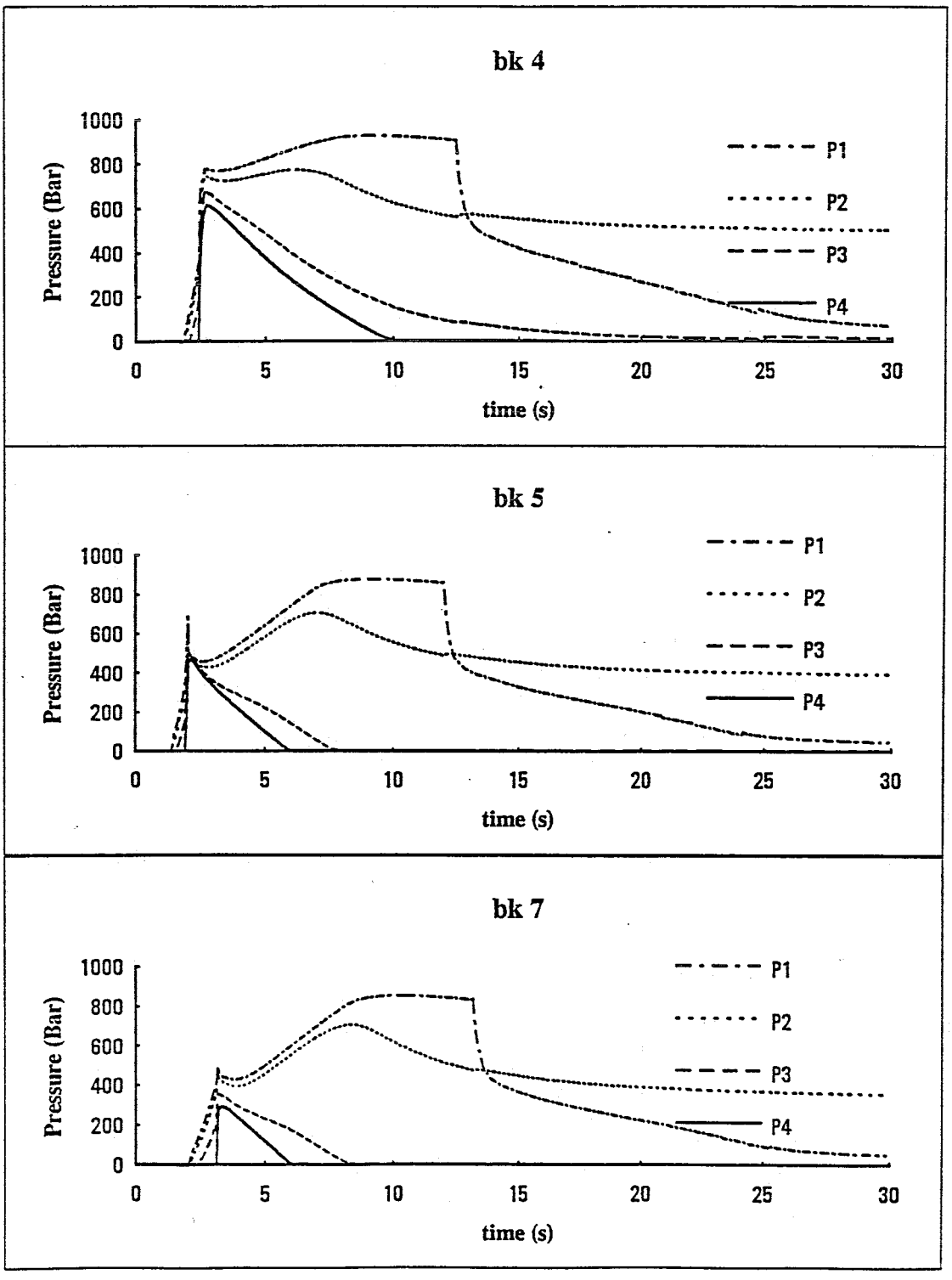
bk 4
Pressure (Bar)
1000
800
600
400
200
0
0
5
10
15
20
25
30
time (s)
P1
P2
P3
P4
bk 5
Pressure (Bar)
time (s)
P1
P2
P3
P4
bk 7
Pressure (Bar)
time (s)
P1
P2
P3
P4

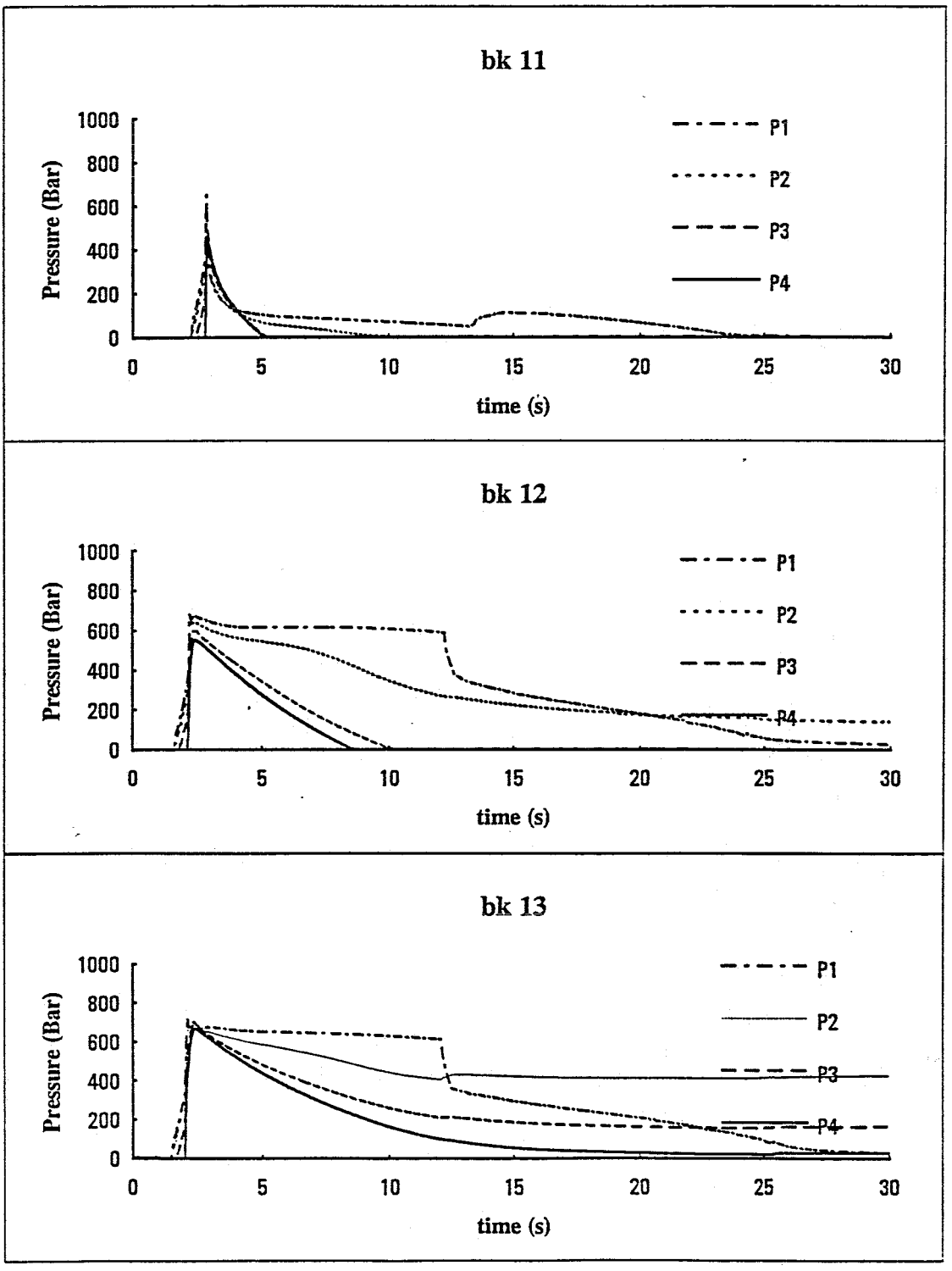
bk 11
Pressure (Bar)
1000
800
600
400
200
0
0
5
10
15
20
25
30
time (s)
P1
P2
P3
P4
bk 12
Pressure (Bar)
1000
800
600
400
200
0
0
5
10
15
20
25
30
time (s)
P1
P2
P3
P4
bk 13
Pressure (Bar)
1000
800
600
400
200
0
0
5
10
15
20
25
30
time (s)
P1
P2
P3
P4

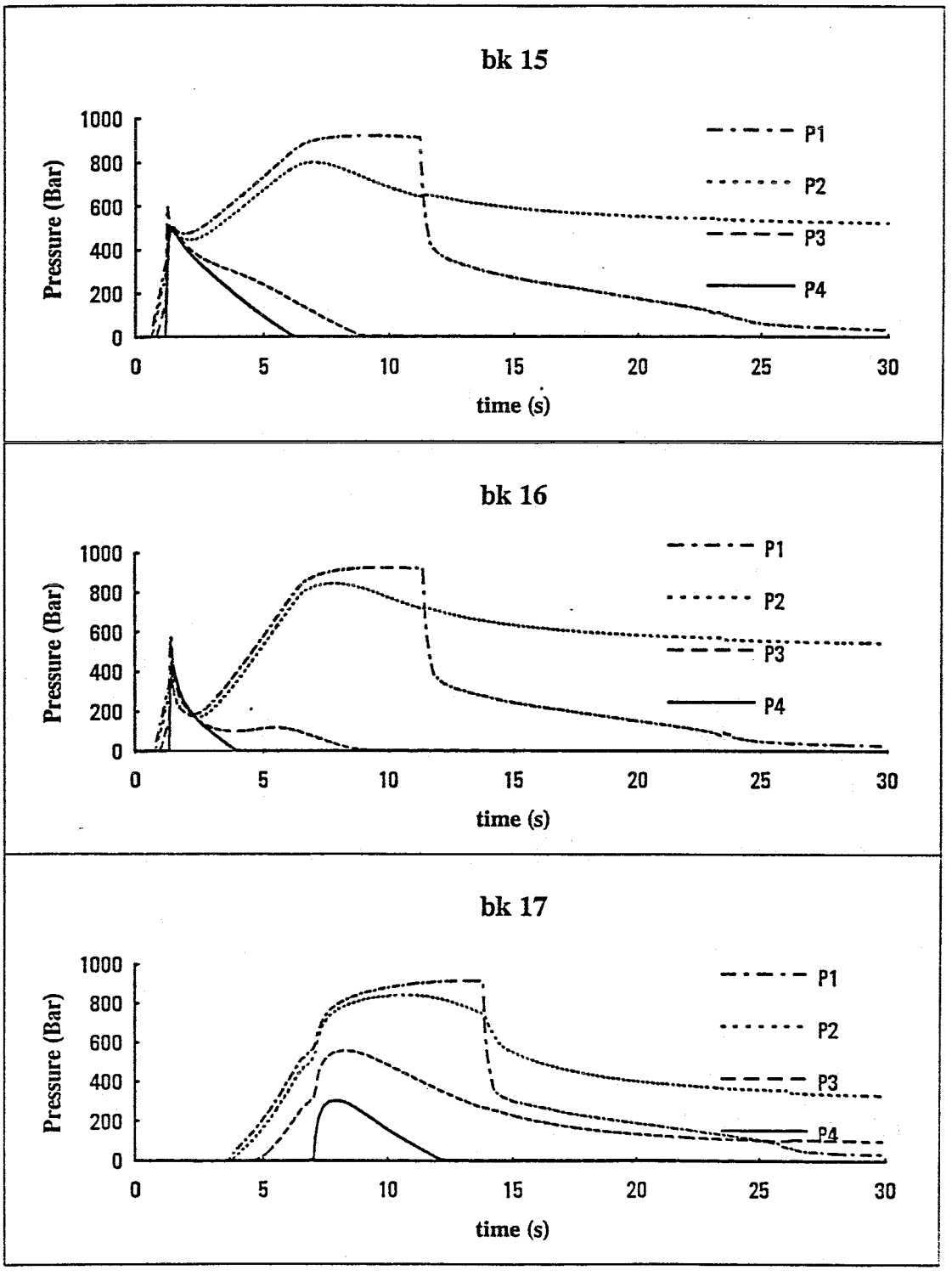
bk 15
Pressure (Bar)
1000
800
600
400
200
0
0
5
10
15
20
25
30
time (s)
P1
P2
P3
P4
bk 16
Pressure (Bar)
1000
800
600
400
200
0
0
5
10
15
20
25
30
time (s)
P1
P2
P3
P4
bk 17
Pressure (Bar)
1000
800
600
400
200
0
0
5
10
15
20
25
30
time (s)
P1
P2
P3
P4

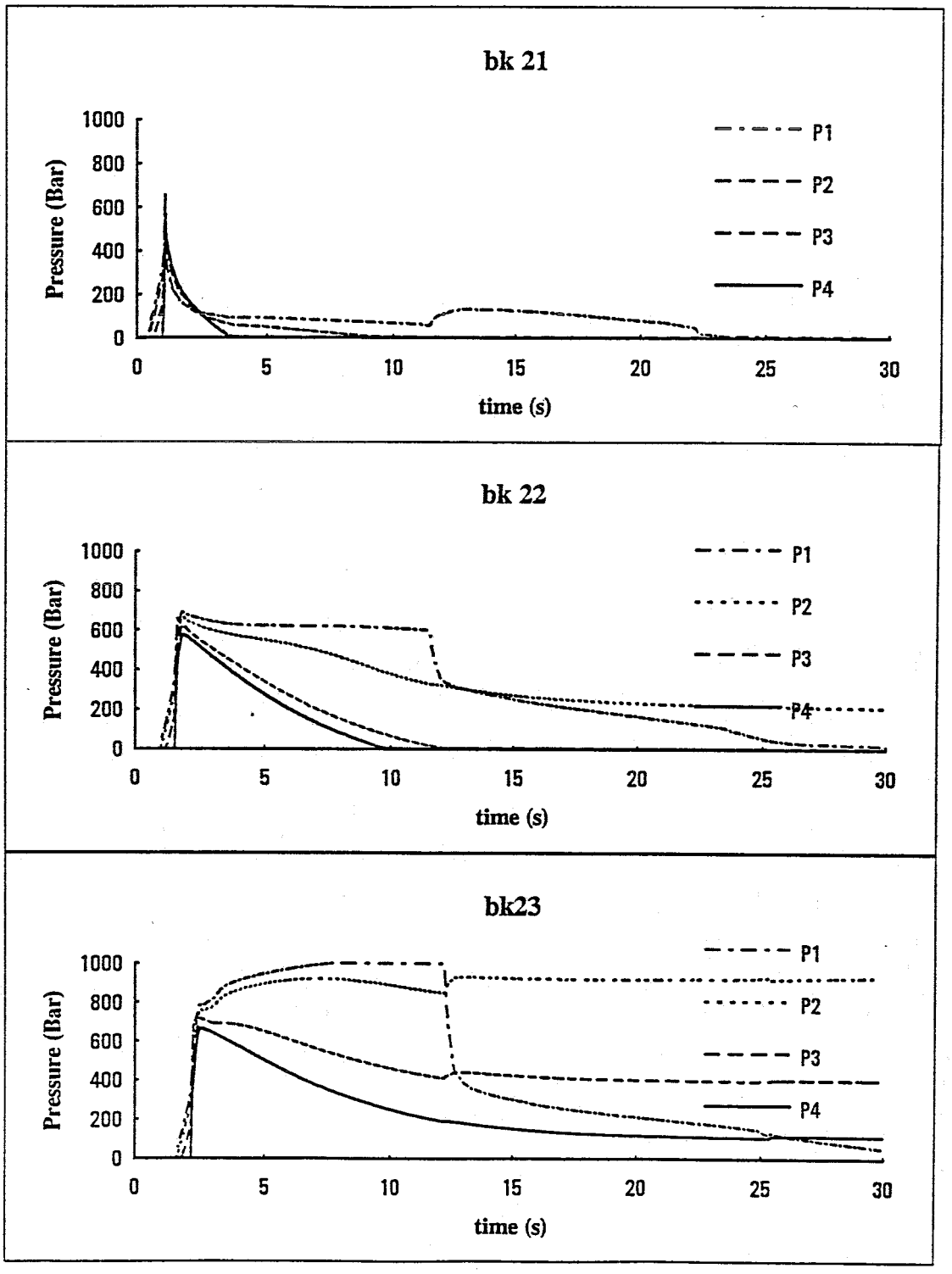
bk 21
Pressure (Bar)
1000
800
600
400
200
0
0
5
10
15
20
25
30
time (s)
P1
P2
P3
P4
bk 22
Pressure (Bar)
time (s)
P1
P2
P3
P4
bk23
Pressure (Bar)
time (s)
P1
P2
P3
P4

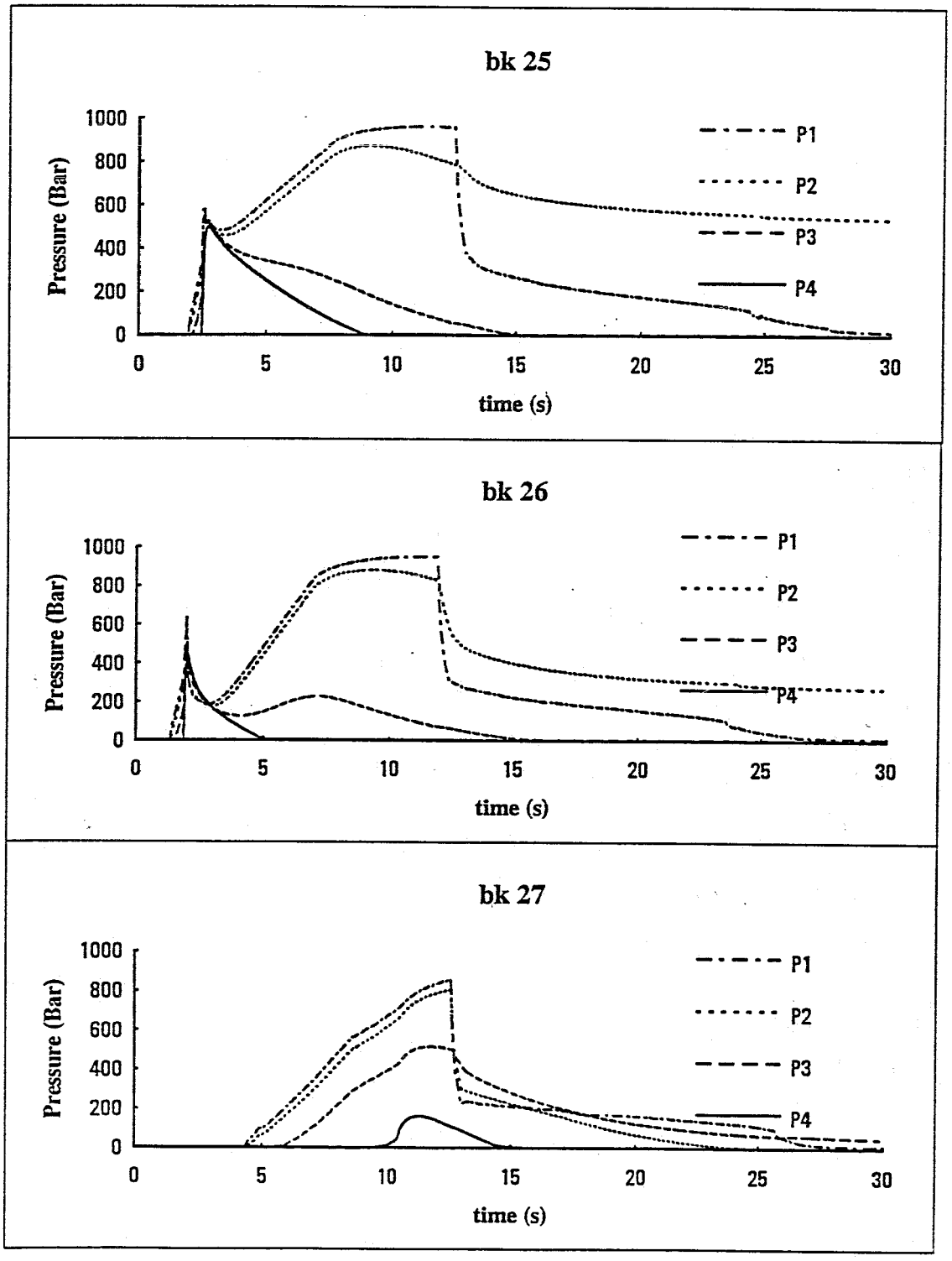
bk 25
Pressure (Bar)
1000
800
600
400
200
0
0
5
10
15
20
25
30
time (s)
P1
P2
P3
P4
bk 26
Pressure (Bar)
1000
800
600
400
200
0
0
5
10
15
20
25
30
time (s)
P1
P2
P3
P4
bk 27
Pressure (Bar)
1000
800
600
400
200
0
0
5
10
15
20
25
30
time (s)
P1
P2
P3
P4